UNIVERSIDADE DE LISBOA
FACULDADE DE CIÊNCIAS
DEPARTAMENTO DE BIOLOGIA VEGETAL

Towards improvement of *Haematococcus pluvialis* cultures by cell sorting and UV mutagenesis

Filipa Faria Rosa

Mestrado em Microbiologia Aplicada

Dissertação orientada por:
Doutor Luís Tiago Guerra
Professora Doutora Ana Tenreiro

2017

Towards improvement of *Haematococcus pluvialis* cultures by cell sorting and UV mutagenesis

Filipa Faria Rosa

2017

This thesis was fully performed at A4F – Algae for Future and Bugworkers Laboratory | M&B – BioISI | Teclabs under the direct supervision of Doutor Luís Tiago Guerra. Professora Doutora Ana Tenreiro was the internal supervisor in the scope of the Master in Applied Microbiology of the Faculty of Sciences of the University of Lisbon.

ACKNOWLEDGMENTS

First of all, I would like to show my gratitude to the administration of A4F – Alga for Future. Not only they gave me the opportunity of carrying out my master thesis but also I was able to work in two laboratories, A4F and Bugworkers Laboratory | M&B – BioISI | Teclabs, thanks to their partnership. It was an exceptional and exclusive experience which I will never forget.

I want to thank Dr. Luis Tiago Guerra, my supervisor at A4F, and Professora Doutora Ana Tenreiro, my supervisor at Bugworkers Laboratory | M&B – BioISI | Teclabs. I am especially grateful for all the knowledge and guidance given along the entire thesis, as well as the availability they showed to help whenever I needed. Not least, thank for the advices, patience, trust and other contributions that allowed the improvement of this work.

I am thankful to all my A4F's colleagues, especially the ones from the laboratory, who gave me all their support and most important, provided me great and unforgettable moments in the laboratory. Not forgetting, my professors and my colleagues from the Bugworkers Laboratory, for answering my questions and clear up my doubts always with the greatest positivity.

To all my friends and family, a huge thanks for being so supportive and always around when needed the most. In particular, a very special thanks to my parents and brother who are the major pillars of my being and who never gave up on my success. Thanks for your support, encouragement, strength and patience.

ABSTRACT

Nowadays, there is an increased interest in biological active compounds derived from natural sources, especially compounds with medical applications, nutrient rich food and feed, and health promoting compounds. Microalgae are a potential valuable resource for a biotech purposes, as new sources of biomolecules such as pigments, lipids, carbohydrates and proteins. Natural pigments have pharmacological properties and have increased marketability of products advantages over synthetic products. Commercial production of natural carotenoids from microalgae is an eco-friendlier and safer approach than synthetic manufacture by chemical procedures. Of several naturally occurring carotenoids, astaxanthin is considered one of the best, being able to protect cells, lipids and membrane lipoproteins against oxidative damage. *Haematococcus pluvialis* is the richest source of natural astaxanthin and is produced at large scale.

The work herein described had the objective to improve *H. pluvialis* strains with an enhanced accumulation of astaxanthin content. For the strain improvement three approaches have been used: (i) screening of different strains to select those with a superior performance; (ii) flow cytometry assisted cell sorting of cells subpopulations with increased astaxanthin production and (iii) random mutagenesis by UV-C irradiation and mutants selection. For this purpose, seven *H. pluvialis* strains were used and a characterization was conducted throughout the 3-steps cultivation experimental strategy: green vegetative growth, induction of astaxanthin accumulation and additional salinity stress stages. This integrative characterization focused on a number of microalgae physiological properties, intending to thoroughly assess the evolution and heterogeneity of their vitality and astaxanthin accumulation capacity.

HP_02 and HP_03 were the most promising selected strains, reaching respectively 3.8 % and 4.4 % (of their DW) of astaxanthin content, and presenting high growth rates of 0.58 day^{-1} and 0.52 day^{-1}. The two strains were submitted to fluorescence activated cell sorting for enrichment of astaxanthin over-producers. Both strains showed similar performances and no specific cell properties and/or stresses responses could be point as particularly relevant. The HP_03 strain was further subjected to random mutagenesis by exposure to UV-C radiation in order to promote heterogeneity in the cell population.

The isolation of cells sub-populations of interest, with high recovery and high degree of purity, was not achieved, due to the homogeneity of the populations of the analyzed strains, and due to technical impossibility of the sorting device. However, it is noteworthy that, flow cytometry allowed the monitoring of astaxanthin content during the induction phase of the culture, and showed that the autofluorescence of this pigment can be a good indicator of its intracellular accumulation and can therefore be monitored in real time by flow cytometry. The results of the preliminary random mutagenesis assay, by exposure to UV-C radiation seem to indicate that this strategy is promising to increase the subpopulation of astaxanthin producing cells. Further similar studies with different strains and additional parameters should be performed to better clarify this subject.

Keywords: astaxanthin; *Haematococcus pluvialis*; flow cytometry; cell sorting; UV mutagenesis.

RESUMO

As microalgas estão a emergir como uma das mais promissoras fontes sustentáveis de biomassa, combustível, alimentação, rações e outros produtos. Estes microrganismos têm um potencial enorme na área da biotecnologia por serem uma fonte valiosa de metabolitos como pigmentos (ex. astaxantina, β-caroteno), proteínas (ex. ficocianina), lípidos (ex. ómega-3, DHA, EPA) e hidratos de carbono. Embora os seus compostos ativos apresentem vantagens relativamente aos produtos sintéticos ou outros produtos de fontes naturais, têm contudo, desvantagens a nível de custos (Borowitzka, 2013; Demirbas, 2011; Milledge, 2010). O maior desafio na aplicação das microalgas para fins comerciais tem sido minimizar os custos de produção e extração dos compostos, devido à complexidade da fase de cultivo e dos processos a jusante (ex. extração dos compostos de valor acrescentado).

Entre os metabolitos de elevado valor acrescentado, a astaxantina (3,3'-dihidroxi-β,β'-caroteno-4,4'diona), carotenoide secundário, é considerada um composto valioso com um elevado número de aplicações, desde sectores alimentares, cosméticos a farmacêuticos. Este pigmento tem como fonte natural microalgas como *Chlorella zofingiensis*, *Chlorococcum*, *Haematococcus pluvialis*, leveduras vermelhas, *Phaffia rhodozyma* e bactérias, *Paracoccus carotinifaciens*. *Haematococcus pluvialis*, é considerada a maior fonte natural de astaxantina, podendo acumular até 6 % do seu peso seco e é a melhor fonte natural de astaxanthina para consumo humano (Ambati *et al*., 2014; Lorenz, 1999; Olaizola, 2003; Yuan *et al*., 2010).

A acumulação de carotenoides secundários, como a astaxantina, é uma característica de resposta ao *stress* de certas microalgas como é o caso de *H. pluvialis*. Quando há privação de nutrientes, aumento da intensidade luminosa, salinidade, etanol e hormonas entre outros fatores desfavoráveis ao crescimento da microalga, esta começa a induzir (Sarada *et al*., 2002a; Su *et al*., 2014; Zhang *et al*., 2014). A fase de indução, também conhecida como fase vermelha, corresponde à produção e acumulação da astaxantina, essencial para *H. pluvialis* sobreviver a condições adversas (Hagen *et al*., 2002; Wayama *et al*., 2013). Devido às flutuações das condições de *stress* que podem ser aplicadas para iniciar o processo de indução, todas as estratégias devem ser otimizadas para que a acumulação de astaxantina seja o mais reprodutível possível. O desenvolvimento de novas tecnologias para produção de microalgas, em sistemas abertos (ex. *raceways*) e sistemas fechados (ex. fotobioreactores), assim como a otimização das condições de cultivo (um ou duas fases de produção) têm maximizado o crescimento e a produção de biomassa, teor de pigmentos e outros produtos, reduzindo os custos de produção à escala industrial (Der Rio *et al*., 2007; Fábregas *et al*., 2001; Shah *et al*., 2016).

Contudo, existem ainda muitos desafios e problemas na produção a grande escala de *H. pluvialis*. A otimização não tem de ser restrita ao melhoramento das condições de cultivo e aos sistemas de produção. O melhoramento do desempenho das estirpes de *H. pluvialis* também tem sido alvo de estudos recentes. Para aumentar o conteúdo de astaxantina acumulado, as células podem ser submetidas a agentes mutagénicos químicos, como etil-metano-sulfanato (EMS) ou N-metil-N-nitro-N-nitrosoguanidina (NTG), ou agentes físicos, como radiação ultravioleta ou raio-X (Chen *et al*., 2003; Kamath *et al*., 2008; Tjahjono *et al*.,1994; Tripathi *et al*., 2001). Mutações mais direcionadas também foram aplicadas a estas microalgas, como modificações genéticas (Forján *et al*., 2015; Sharon-Gojman *et al*., 2015).

O trabalho desenvolvido no âmbito desta tese teve como principal objetivo o melhoramento de estirpes de *H. pluvialis*, pertencentes à coleção de microalgas da empresa A4F, para aumentar o teor intracelular

de astaxantina. Para o melhoramento das estirpes foram utilizadas três abordagens: (i) caracterização de diferentes estirpes para posterior seleção daquelas que apresentaram desempenho superior; (ii) separação física (*cell sorting*) de subpopulações de células com aumento da produção de astaxantina, por citometria de fluxo e (iii) mutagénese aleatória por irradiação com UV-C e seleção de mutantes.

Neste trabalho foram inicialmente utilizadas sete estirpes de *H. pluvialis* (HP_01 to HP_07) cultivadas numa estratégia experimental em três fases: na primeira fase de crescimento vegetativo ou fase verde, as diferentes estirpes foram crescidas em condições ótimas durante 7 dias, avaliando-se e comparando as taxas de crescimento e produtividade da biomassa; na segunda fase de indução ou fase vermelha, aplicaram-se dois fatores de stress, privação de nutrientes e aumento da intensidade luminosa (150 $\mu mol.m^{-2}.s^{-1}$), durante 17 dias, analisando-se a produtividade e a acumulação máxima de astaxatina nas diferentes estirpes; na terceira fase aplicou-se um *stress* salino adicional, analisando-se o seu impacto na biomassa e no conteúdo máximo de astaxantina das culturas já induzidas. Esta caracterização integrativa enfocou um número de propriedades fisiológicas das microalgas, com a intenção de avaliar completamente a evolução e heterogeneidade de sua vitalidade e capacidade de acumulação de astaxantina. Os parâmetros avaliados foram: contagem de células, peso seco, produtividade e viabilidade de biomassa e análise de pigmentos.

Os resultados obtidos no decurso deste trabalho permitiram caracterizar as diferentes estirpes de *H. pluvialis* e selecionar as que apresentaram as melhores características relativamente à taxa de crescimento e produtividade de biomassa na fase de crescimento, e com especial interesse à sua produtividade e teor em astaxantina na fase de indução. Das sete, destacaram-se as estirpes HP_02 e HP_03, que durante a fase de crescimento apresentaram elevadas taxas de crescimento (0,52 e 0,58 dia^{-1}, respetivamente) e produtividades similares de biomassa comparativamente às outras estirpes (0,27 e 0,22 $g.L^{-1}.dia^{-1}$, respetivamente). HP_02 e HP_03, obtiveram o maior conteúdo de astaxantina acumulado (3,8 % e 4,4 % respetivamente), e registaram produtividades de astaxanina elevadas, (2,31 e 2,58 $mg.g^{-1}.dia^{-1}$ respetivamente), superiores às outras estirpes estudadas. As duas estirpes foram submetidas a *cell sorting* para enriquecimento de sobre-produtores de astaxantina. Ambas as estirpes apresentaram desempenhos semelhantes e não foram consideradas particularmente relevantes propriedades específicas das células. A estirpe HP_03 foi ainda sujeita a mutagénese aleatória por exposição à radiação UV-C de modo a promover a heterogeneidade na população celular.

Os pigmentos fotossintéticos presentes nas microalgas são clorofilas e carotenóides, e a sua concentração intracelular depende das condições de cultivo. Esta concentração está linearmente correlacionada com a fluorescência dos pigmentos, o principal componente da fluorescência endógena (autofluorescência) (Hyka *et al*., 2013). Assim, a intensidade de autofluorescência foi utilizada para a identificação e quantificação de pigmentos de microalgas por citometria de fluxo. Esta metodologia permitiu ainda detetar alterações no estado fisiológico das células; a morfologia, incluindo tamanho e complexidade celular dependem das condições de cultivo e estão correlacionadas com os dois sinais de dispersão da luz, medidos por citometria, nomeadamente dispersão direta (FSC) e ortogonal (SSC).

A acumulação de astaxantina das 7 estirpes, foi monitorizada por citometria de fluxo, no início e ao longo da fase de indução, assim como foi seguida a evolução do estado fisiológico das células. É de salientar que os resultados da quantificação de astaxantina por citometria de fluxo (valores médios das intensidades de fluorescência) foram consistentes com os determinados pelo método de extração de pigmentos totais, confirmados pela forte correlação linear encontrada ($r = 0,98$) entre o conjunto completo de valores dos dois parâmetros. Demonstrou-se assim que, a autofluorescência da astaxantina é um bom indicador da sua acumulação intracelular, podendo ser monitorizada em tempo real por citometria de fluxo.

Para concluir a fase de caracterização das estirpes, os resultados obtidos após adição de NaCl (10 g/L) mostraram que o aumento do conteúdo de astaxantina não é estatisticamente significativo, à exceção de HP_01 que obteve um aumento de 2,5 % para 3,4 % ($p < 0,001$). A aplicação do *stress* salino adicional, ainda que apenas durante um curto período de tempo, 1 a 2 dias, determinou um aumento do teor de astaxantina, começando as culturas a perder biomassa após o terceiro dia, e como tal teve efeitos negativos no conteúdo de astaxantina acumulado. A maior produtividade global de astaxantina foi obtida pelas estirpes HP_02 e HP_03, atingindo 1,63 e 1,88 $mg.g^{-1}.dia^{-1}$, respetivamente. Este valor foi baseado no tempo essencial para as estirpes alcançarem o valor máximo de astaxantina, incluindo as duas fases de cultivo durante 24 dias.

A partir das culturas selecionadas, HP_02 e HP_03, o isolamento de subpopulações de células de interesse, com alta recuperação e alto grau de pureza, não foi alcançado, devido à homogeneidade das populações das estirpes analisadas, e devido à impossibilidade técnica do dispositivo de *sorting*.

Como terceira abordagem para o melhoramento das estirpes, a HP_03 foi selecionada, realizou-se mutagénese aleatória por exposição à radiação ultravioleta (UV-C), criando condições propícias a que as células sofressem alterações genéticas de modo a potenciar a produção de astaxantina. O efeito letal da exposição à radiação foi estudado analisando a viabilidade celular por citometria de fluxo, usando como fluoróforo um oxonol [$DiBAC_4(3)$], que responde ao potencial de membrana. Os resultados obtidos permitiram seguir a evolução da viabilidade celular com o aumento do tempo de exposição à radiação, observando-se uma despolarização progressiva da membrana, que terminou ao fim de 100 s de exposição por uma dissipação generalizada do potencial. No entanto, nos resultados obtidos pela análise de citometria de fluxo, não foi notável um aumento da heterogeneidade populacional, mantendo-se a dificuldade da realização do *sorting* das células com maior conteúdo de astaxantina. Este ensaio preliminar de mutágenese aleatória apresentou resultados promissores, na medida em que um dos mutantes isolados, Mut 2, atingiu valores superiores de astaxantina, 4,1 % por peso seco, relativamente ao controlo que obteve 3,1 % de astaxantina, para o mesmo período de tempo.

Uma vez que as estirpes selecionadas apresentaram um desempenho análogo e uma homogeneidade populacional, torna-se difícil identificar propriedades celulares ou respostas ao *stress* que possam ser particularmente relevantes para o melhoramento das estirpes com vista a uma maior acumulação de astaxantina. Deverão realizar-se novos estudos com recurso a estirpes com maior heterogeneidade, que possibilitem o isolamento das células com as propriedades desejadas, e as configurações do citómetro de fluxo e do dispositivo de *sorting* devem ser otimizadas de modo a permitir separação física (*cell sorting*) de subpopulações de células com aumento da produção de astaxantina, com alta recuperação e alto grau de pureza.

Palavras-chave: astaxantina; *Haematococcus pluvialis*; citometria de fluxo, *cell sorting*; mutagénese por UV.

INDEX

LIST OF FIGURES

LIST OF TABLES

LIST OF EQUATIONS

1 – INTRODUCTION

1.1. MICROALGAE OVERVIEW

1.1.1. Microalgae playing an important role

Microalgae are unicellular, colonial or filamentous, aquatic organisms that convert sunlight, nutrients and carbon dioxide into biomass via photosynthesis. Microalgae are one of the most primitive plants, consisting of the base of food chain of all aquatic ecosystems and the primary producers on earth. It can be grown almost anywhere, fresh water, salt-water and even on sewage and hypersaline waters. Around 200,000 species of microalgae are estimated to exist, but only a limited number, about 30,000, have been studied and analyzed (Mata *et al*., 2010; Sing and Saxena, 2015). Microalgae consist of a large and heterogeneous group of microorganisms, distinguished according the basic cellular structure, life cycle and pigment composition. The most important classes or categories of microalgae in terms of their abundance are: diatoms (*Bacillariophyceae*); green (*Chlorophyceae*); blue-green algae or cyanobacteria (*Cyanophyceae*); golden (*Chrysophyceae*); and red algae (*Rhodophyceae*) (Bharathiraja *et al*., 2015; Sing and Saxena, 2015; Vassilev and Vassilev, 2016).

Microalgae photosynthetic mechanism is similar to that of terrestrial plants, however, it has specific advantages over; it presents higher photosynthetic efficiency, since microalgae, during cellular metabolism, can convert more solar energy (4 - 7.5 %) than land plants (0.5 %). Moreover, microalgae present higher biomass production and faster growth, with growth rates of less than 24h. Microalgae also depend upon fewer resources than land plants, do not require fertile land or food crops, and processing consumes less energy than the land plants need (Raheem *et al*., 2015; Sing and Saxena, 2015). Although, its cultivation is very challenging, once variations in light, temperature, pH, salinity, qualitative and quantitative nutrient profiles, dissolved oxygen, among others, will affect the growth and the quality of microalgae. These conditions can be modified to accomplish high yields and reduce production costs (Tran *et al*., 2015).

To benefit the most from microalgae, since its isolation up to its large-scale production, several stages have to be studied, and microalgae potential is acquired step by step. The increasing concern for a better life quality, by consuming from natural sources and usage of renewable resources, is leading to a high investment in microalgae business and an increasing research for its biotechnological applications (Bharathiraja *et al*., 2015; Markou and Nerantzis, 2013; Vassilev and Vassilev, 2016).

1.1.2. Microalgae products & economic interests

Microalgae are a potential resource for biotechnological purposes as new sources of biomolecules such as pigments, lipids, carbohydrates and proteins. Microalgae in their natural environment, have adapted in order to inhabit a wide range of environmental conditions and habitats. Therefore, due to their variety of metabolic pathways, these microorganisms can produce an enormous diversity of compounds. Microalgae biomass from different strains can be processed and their active form from its compounds, such as pigments (*e.g.* β-carotene), antioxidants (*e.g.* astaxanthin), proteins (*e.g.* phycocyanin), and polyunsaturated fatty acids (*e.g.* omega-3, DHA, EPA) can be extracted to commercialize (Borowitzka, 2013; Demirbas, 2011).

Although the current key commercial applications appear to be food additives and fuel, microalgae and its compounds have a tremendous range of applications. These may have advantages over synthetic products or products obtained from natural sources, but may have a cost disadvantage. These characteristics make them promising microorganisms with possible impact, on the chemical, pharmaceutical, cosmetic, energetic and on nutritional sectors (Table 1.1). The challenge in the application of microalgae for commercial purposes is to focus on these products with large market and profit, for which the use of microalgae is a clear competitive advantage (Milledge, 2010).

Table 1.1 – Examples of microalgae products and applications. (Adapted from Bharathiraja *et al*., 2015 and Enzing *et al*., 2014).

Species	Product	Area of application	Price (€/*Kg*)
Spirulina	Phycobiliproteins; γ-linolenic acid	Health care; cosmetics	11-35
Chlorella	Protein isolates	Aquaculture; health care	36-50
Dunaliella salina	β-carotene	Health care; cosmetics	215-2150
Aphanizomenon *flos-aquae*	Nutritional additive	Human nutrition	-
Haematococcus pluvialis	Carotene; astaxanthin	Health care	501-7150
Cryptheconidium cohnii	Dhydroxy acenote oil	Health care; nutrition	43
Nannochloropsis	Eicosapentaenoic acid; Biofuel	Human nutrition; energy	-
Porphyridium	Arachidonic acid	Human nutrition	-
Cryptocodinium	Docosahexaenoic acid	Human nutrition	-

The first report of human consumption of microalgae was in the 16th century with the harvest of *Spirulina (Arthrospira)* from Lake Texcoco by the Aztec people, and latter of Lake Chad by Kanembu population. During the natural Spirulina bloom, the populations collected and dried microalgae for later consumption as dried cakes. Nutritional properties of *Spirulina* showed an exceptionally high protein content, of the order of 60–70 % of its dry weight (Abdulqader *et al*., 2000; Ahsan *et al*., 2008). However, the industrial scale production of microalgae only began in the 1960s, in Japan with *Chlorella* production for human consumption. *Chlorella vulgaris* presents a total protein content up to 60% dry weight. It is considered to have a high protein nutritional quality according to the standard amino acid profile for human nutrition proposed by the World Health Organization (WHO) and the Food and Agricultural Organization (FAO) (Safi *et al*., 2014). This was followed in the 1970s by the commercialization of *Spirulina*, which is an excellent source of C-phycocyanin, followed in the 1980s by *Dunaliella salina*, source of β-carotene and later source of glycerol (Ben-Amotz and Avron, 1982; Spolaore *et al*., 2006) and astaxanthin from *Haematococcus pluvialis* in the 1990s (Lorenz and Cysewski, 2000). Thus, microalgae biotechnology industry has been growing and diversifying significantly.

However, the microalgae products currently on the market are still limited. The main limiting factor for the development of the markets is the production costs. The actual costs are related to the complexity of the cultivation phase and the downstream processes (extraction of the high-value compounds). The technical innovation and the market demand will result in further major advances and in an expansion of the commercially available products. Besides, efforts in improving the efficiency of systems and production operation are in progress to allow the cultivation of a larger diversity of microalgae. Nowadays, nutrition education programs could improve the microalgae products consumption. The main commercial product appears to be ‘‘health care’’ or “nutrition” that may produce health benefits, but may be subject to fashion and the current tendency. Also, to increase the microalgae products should be done a revision of the Novel Food Regulation. The complexity of the regulation on novel foods makes

it difficult the authorization of microalgae based products on the market (Milledge, 2010; Podola *et al*., 2016; Spolaore *et al*., 2006; Vigani *et al*., 2015).

Alternative sources, as chemical synthesis products, are the major competitors of several of the microalgae products, especially carotenoids. According to BCC research press release (BCC research), the global carotenoids market generated about $1.2 billion in 2010, with the bulk of the carotenoids being produced by chemical synthesis (Borowitzka, 2013). In 2018, that value is projected to surpass $1.4 billion, increasing at an eight-year Compound Annual Growth Rate (CAGR) of 2.3 %. The global market for carotenoids comprise principally ten products: β-carotene, lutein, astaxanthin, capsanthin, annatto, canthaxanthin, lycopene, β-apo-8-carotenal, zeaxanthin, and β-apo-8-carotenal-ester (Figure 1.1).

The higher quality of microalgae compounds compared to the corresponding synthetic sources, is mainly due to their chemical conformation which is much more efficient than the synthetic variants. The products of high added value obtained from microalgae are subject to a range of rules and regulations affecting the production process. The concerns of production process are incremented when it is intended for human or animal nutrition. The alternative sources present a challenge to producers of microalgae-derived products, which have either to compete on price, or differentiate themselves from the synthetic source in the market place, in order to be able to be sold at a higher price. The manufacturing processes required to produce natural carotenoids are sophisticate and suffered a high development over the past years. Introduction of new manufacturing technologies is leading to a price reduction across most products allowing the preference for natural sources instead of synthetic. From this, biotechnology will play an important role in the near future, especially in production systems, as it can help to increase the productivity and reduce the production costs of micro-algae products (Borowitzka, 2013; Enzing *et al*., 2014; Guedes *et al*., 2011).

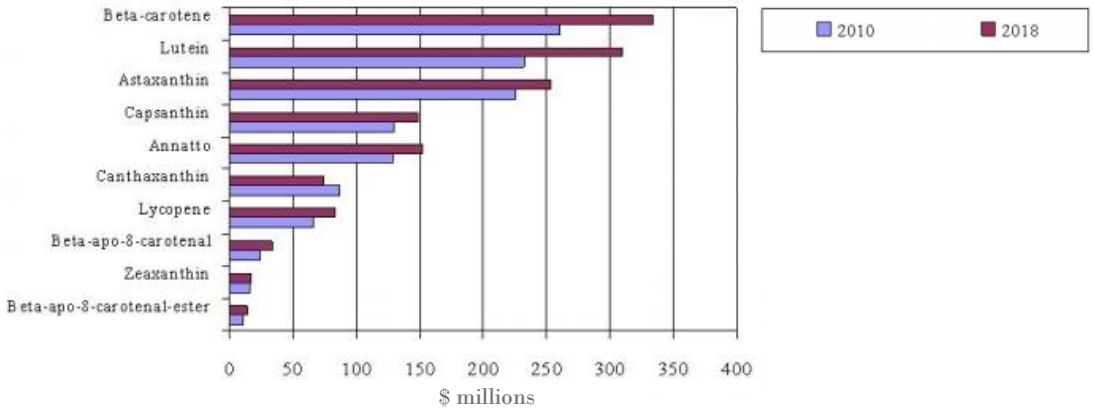

Figure 1.1 – Global carotenoids market value by product type. Estimative of evolution of carotenoid market from 2010 to 2018 ($ millions). Extracted from BCC Research.

1.2. ASTAXANTHIN PIGMENT

Nowadays there is an increased interest in biological active compounds derived from natural sources, especially the ones that can act on molecular targets, which are involved in some diseases. Astaxanthin (3,3'-dihydroxy-β,β'-carotene-4,4'dione) a compound of highly interest, has unique chemical properties based on its molecular structure, derived from lycopene. It is a hydrocarbon that contains two terminal ring systems joined by a chain of conjugated double bonds or poliene system (Figure 1.2) (Guerin *et al*., 2003). Its structure explains its unique chemical features, such as the ability to be esterified, a higher anti-oxidant activity and a more polar configuration than other carotenoids. Astaxanthin, a secondary carotenoid that results from secondary metabolism, belongs to the family of xanthophyll and it has a

stronger antioxidant activity when compared to β-carotene or α-tocopherol. It is proposed to be a super vitamin E and it can easily cross blood brain barrier in mammals, having proprieties that are believed to have a key role in the medicinal, pharmaceutical and food industries. (Goswami *et al*., 2010; Miki, 1991).

Of several naturally occurring carotenoids, astaxanthin is considered one of the best being able to protect cells, lipids and membrane lipoproteins against oxidative damage (Ambati *et al*., 2014). Numerous studies (Ambati *et al*., 2014; Guerin *et al*., 2003; Kidd, 2011; Yamashita, 2013; Yuan *et al*., 2011) have shown that astaxanthin has potential health-promoting effects in the prevention and treatment of various diseases, such as cancers, chronic inflammatory diseases, metabolic syndrome, diabetes, cardiovascular diseases, gastrointestinal diseases, liver diseases, neurodegenerative diseases, eye diseases, skin diseases, exercise-induced fatigue, male infertility, and renal failure.

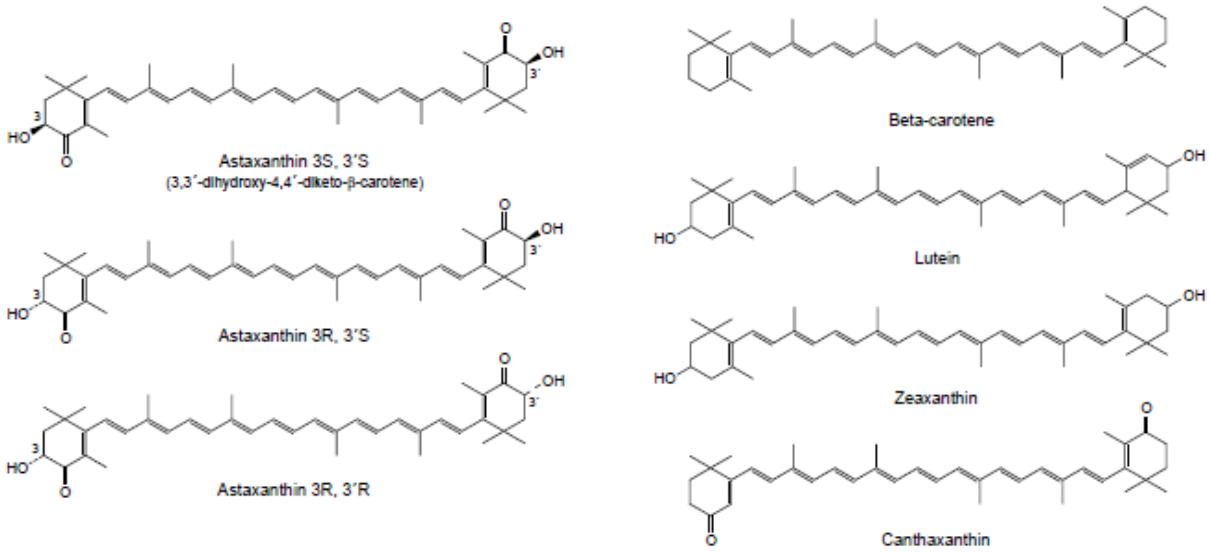

Figure 1.2 – Molecular structure of different carotenoids: the three stereoisomers of astaxanthin, β-carotene, lutein, zeaxanthin and canthaxanthin. Extracted from Guerin *et al*., 2003.

Astaxanthin shares many of the metabolic and physiological functions attributed to carotenoids, since it is closely related to other carotenoids, such as β-carotene, zeaxanthin and lutein (Figure 1.2) (Goswami *et al*., 2010; Guerin *et al*., 2003). There are three stereoisomers for astaxanthin: two enantiomers (3R, 3'R and 3S, 3'S) and a meso form (3R, 3'S). Of all isomers, the 3S, 3'S is the most abundant in nature and different organisms produce astaxanthin in different stereoisomeric ratios. Esterified astaxanthin may increase biological activities especially since it can be easily absorbed into the metabolism, when compared to its free form. The stereoisomer 3S, 3'S in the esterified form (mono and di-esters) is predominantly found in *Haematococcus pluvialis*, while the 3R, 3'R stereoisomer in the unesterified form is found in *Phaffia rhodozyma*. Synthetic astaxanthin is produced as the unesterified xanthophyll and as a 1:2:1 mixture of the three stereoisomers: 3S, 3'S, 3R, 3'S and 3R, 3'R (Ambati *et al*., 2014; Higuera-Ciapara *et al*., 2006).

Astaxanthin is found in microalgae, microorganisms and aquatic animals, *i.e.* many types of seafood, including salmon, trout, red sea bream, shrimp and lobster, as well as in birds such as the flamingo and the quail. There are diverse natural sources of astaxanthin, such as microalgae *Haematococcus pluvialis*, *Chlorococcum*, *Chlorella zofingiensis*, red yeast, *Phaffia rhodozyma* and bacteria, *Paracoccus carotinifaciens*. *Haematococcus pluvialis* is considered the richest source of natural astaxanthin (up to

6 % dry weight) as well as the best sources of astaxanthin for human consumption (Ambati *et al*., 2014; Lorenz, 1999; Olaizola, 2003; Yuan *et al*., 2010).

1.2.1. Biochemistry and biological activity of astaxanthin

An unavoidable consequence of aerobic metabolism is the production of reactive oxygen (ROS) and nitrogen (RNS) species. In microalgae, ROS are always formed by the leakage of electrons onto O_2 from the electron transport activities of chloroplasts, mitochondria and plasma membranes or as a byproduct of various metabolic pathways. All ROS are extremely harmful to organisms at high concentrations and its enhanced production during environmental stresses can cause peroxidation of lipids, oxidation of proteins, damage of nucleic acids and enzyme inhibition, ultimately leading to cells death (Ambati *et al*., 2014).

Due to the polyene chain, astaxanthin has an antioxidant activity by quenching single oxygen and scavenging radicals to terminate chain reactions. Specific physicochemical interactions of antioxidant compounds with membranes are responsible for their antioxidant properties and their biologic benefits, such as its transmembrane orientation which facilitates electron shuttling. The transmembraneous alignment of polar carotenoids provides exposure of the polar (hydrophilic) ends of the molecule to the internal cytoplasm and to the aqueous environment external to the cell (or the mitochondrial matrix and the intermembrane space of mitochondria), potentially facilitating electron transfer via the double bonds of the carbon scaffold of the compound (Figure 1.3) (Ambati *et al*., 2014; Kidd, 2011; Pashkow *et al*., 2008; Yuan *et al*., 2011).

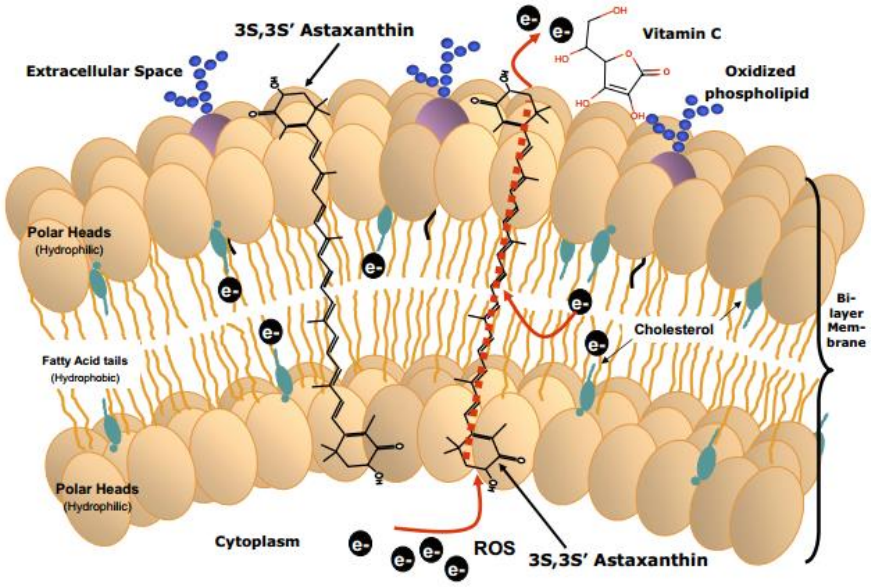

Figure 1.3 – Transverse cell membrane orientation of 3S,3S' astaxanthin. The polar end groups overlap the polar boundary zones of the membrane, while the nonpolar middle fits the membrane's nonpolar interior. The dashed red line speculatively indicates the conduction of electrons along the astaxanthin molecule, possibly to vitamin C or other antioxidants located outside the membrane. Extracted from Pashkow *et al*., 2008.

1.2.2. Natural *vs* synthetic source of high value molecule: Astaxanthin

Natural pigments have pharmacological properties and have increased marketability advantages over synthetic products. The commercial production of natural carotenoids from microalgae is an eco-friendlier and safer approach than synthetic manufacturing by chemical processes (Aberoumand, 2011; Tuli *et al*., 2014). Currently, astaxanthin accounted for $226 million in 2010 and will be worth $253 million in 2018, a CAGR of 1.4 % (BCC Research). However, 95 % of this market consumes synthetic

astaxanthin. Natural products make the synthetic pigments less desirables, since are derived from petrochemical sources raising issues related to food safety, pollution, and sustainability. Therefore, the chemical astaxanthin is only allowed to be used in aquaculture, not in human consumption or animal feed (Lemoine and Schoefs, 2010; Li *et al*., 2011; Lorenz and Cysewski, 2000). Due to consumers' ability to differentiate between the benefits of natural pigments and hazardous effects of synthetic pigments have been greatly boosted the application of microbial pigments as food additive (Nigan and Luke, 2016).

There are three key areas where further improvements are required for a better implementation of microalgae products: (i) minimization of capital and operational costs; (ii) enhancement of cultivation efficiency; and (iii) astaxanthin isolation and purification. This will lead algae companies to successful commercial implementation. Since US Food and Drug Administration (FDA) granted "Generally Recognized As Safe" status (GRAS) astaxanthin from *H. pluvialis*, biotechnological innovation and continuous research are walking side by side to enhance microalgae production technology and strain improvement (*e.g.* genetic engineering), into a sustainable source of food/feed commodities, with enhanced yields of the desired products. (Bhosale, 2004; Pulz and Gross, 2004; Shah *et al*., 2016; Vigani *et al*., 2015).

1.3. *HAEMATOCOCCUS PLUVIALIS*

Haematococcus pluvialis (hereafter referred to as *H. pluvialis*) is the microorganism used for the work of this thesis.

1.3.1. Taxonomy, Morphology & Life cycle

H. pluvialis is a freshwater, unicellular, biflagellate green microalgae. Its scientific classification, originally described by Flotow (1844), is presented in Table 1.2 (Algabase).

Table 1.2 – Taxonomic classification of *H. pluvialis* Flotow. From Algabase.

Domain	**Eukaryota**
Kingdom	Plantae
Subkingdom	Viridiplantae
Phylum	Chlorophyta
Class	Chlorophyceae
Order	Chlamydomonadales
Family	Haematococcaceae
Genus	*Haematococcus*
Species	*Haematococcus pluvialis*

H. pluvialis is adapted to a diverse range of environmental and climate conditions, being distributed in many fresh water habitats worldwide. It is capable of surviving in adverse conditions due to its ability to encyst, such as high light intensity, salt concentration, temperature, water availability and other adverse conditions (Proctor, 1957). This microalgae is frequently found in temperate regions around the world, like Europe, America and Africa (Pringsheim, 1966). However, it had been found to withstand adverse conditions revealing its presence at: low temperatures (4 - 10 °C), in Blomstrandhalvøya Island (Svalbard) (Klochkova *et al*., 2013); at high salinities (up to 25 ‰) on coastal rocks on Kost'yan Island, White Sea (Chekanov *et al*., 2014) and at a dried fountain near Rozhen village Blagoevgrad in Bulgaria (Gacheva *et al*., 2015).

Several ultrastructural changes occur during *H. pluvialis* life cycle which may be divided in four stages: (i) vegetative cell growth; (ii) encystment (vegetative to immature cyst cells); (iii) maturation (immature to mature cyst cells) and (iv) germination (mature cyst to vegetative cells) (Kobayashi *et al*., 1997a). In the life cycle four types of cells are produced (Figure 1.4): macrozooids (large, flagellated); microzooids (small, slender and flagellated); palmella forms (non-motile) and aplanospores (large, red hematocysts with a resistant cellulose wall). Cellular structure and chemical changes allow *H. pluvialis*, under nutritional and environmental factors, to transform from green flagellated cells into red cell, aplonospores, and *vice versa* (Hagen *et al*., 2002).

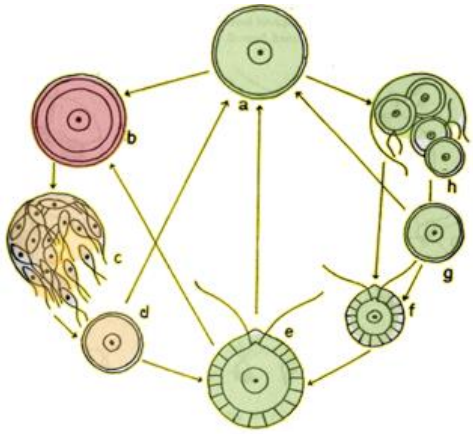

Figure 1.4 – Life cycle of *H. pluvialis*. a) Adult palmelloid cell; b) Aplanospore; c) cell division, microzoids released; d) Young palmelloid cell; e) Adult macrozoid; f) Young macrozoid; g) Palmelloid cell; h) cell division, microzoids and palmella cells released (Adapted from Elliot, 1934).

When a culture is performed with fresh medium, macrozooids (zoospores) predominate in the vegetative growth stage. Cells are spherical, ellipsoidal, or pear-shaped with two flagella of equal length emerging from anterior end, and a cup-shaped chloroplast with numerous, scattered pyrenoids (Kobayashi *et al*., 1997a). Macrozooid cells are between 8 and 20 μm long with a distinct gelatinous extracellular matrix with a median tripartite crystalline layer (Figure 1.5A) (Hagen *et al*., 2002). These cells might divide asexually, by mitosis, into 2 to 32 daughter cells (Figure 1.5B) (Wayama *et al*., 2013). As soon as environmental or culture conditions change inducting stress, macrozooids develop into a non-motile palmella form by losing their flagella while expanding the cell size. The transformation into palmella cells is characterized by the formation of a new two-layered amorphous, primary wall and simultaneously, the tripartite crystalline layer decomposition (Figure 1.5A) (Hagen *et al*., 2002).

Through the continued environmental or cultural stress (*e.g.* nutrient starvation) the encystment process will continue. *H. pluvialis* turned into greenish-orange cells (Figure 1.5C), which can be referred as intermediate stage cells. In the aplanospore or cyst stage (Figure 1.5D) astaxanthin accumulates and cells form cysts. At this stage, further morphogenesis occurs. There is a formation of a voluminous multilayered cell wall, which enhances their tolerance against environmental impact (Damiani *et al*., 2006; Hagen *et al*., 2002). Along the transition to aplanospore cells, a large amount of astaxanthin is synthesized in lipid vesicles in the cytoplasm, in a way to storage carbon, energy and prevention from oxidative stress. The maturation of cysts is accompanied by the degradation of chloroplasts, remaining a low percentage that will play a role in the recovery when environmental conditions improve (Collins *et al*., 2011; Li *et al*., 2008; Triki *et al*., 1997; Wayama *et al*., 2013). *H. pluvialis* has shown sexual and asexual reproduction. However, little is known about its sexual life cycle. Triki *et al*., 1997, had reported that gametogenesis is seen when cultures are recovering from an induction period. Gametocyst may contain 32 or 64 gametes, designated microzoids, which are equal to asexual reproduction flagellated cells, despite their smaller size (10 μm) and rapid swim after release from gametocysts.

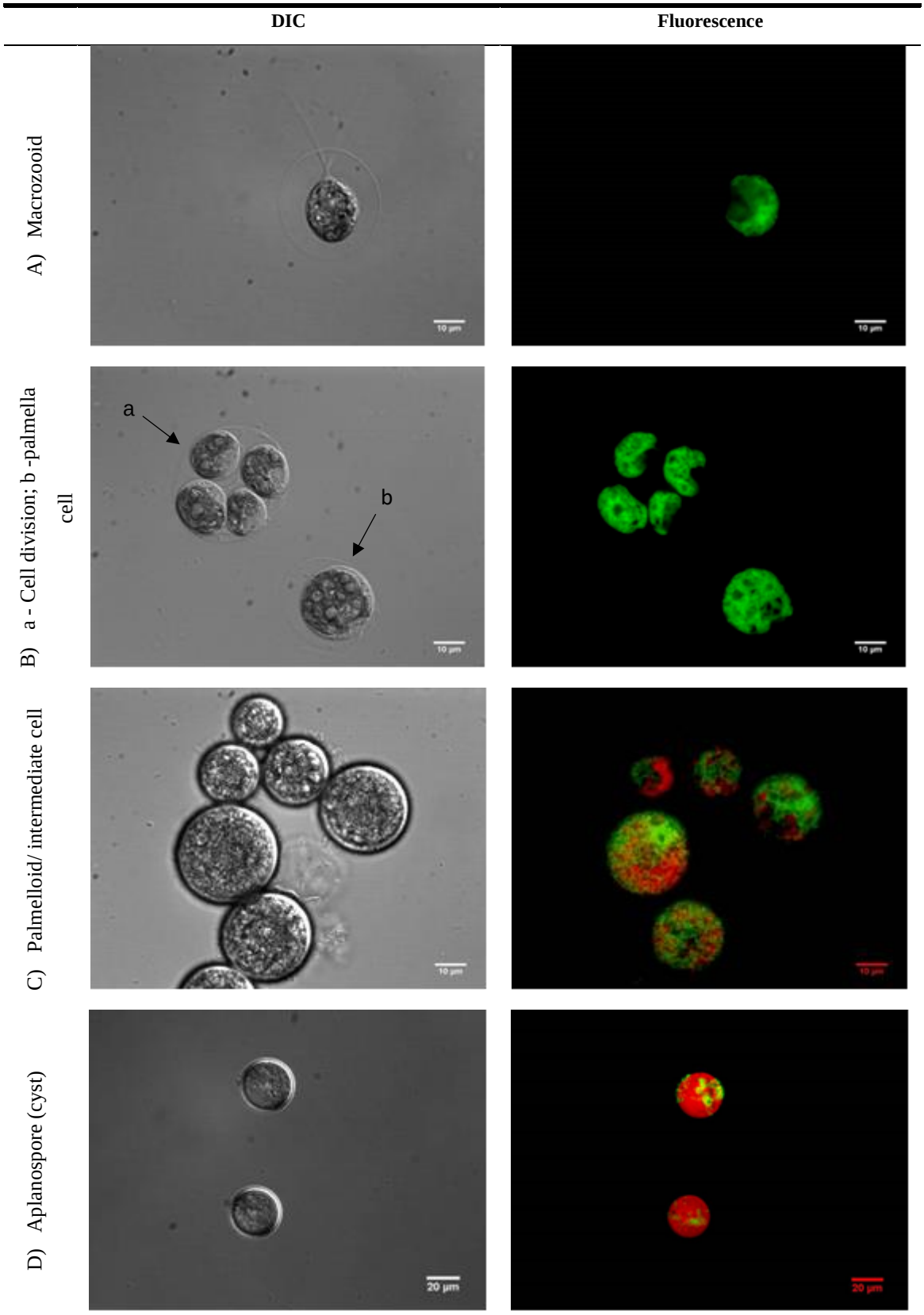

Figure 1.5 – Light (DIC) and fluorescent microscopy images of *H. pluvialis* life cycle. A) Green vegetative motile cell, macrozooid; B) Cell division and transformation of a motile cell into a palmella cell; C) Intermediate cell, beginning astaxanthin accumulation; D) Aplanospore cell, cyst with astaxanthin accumulation. In fluorescent imagens, green color correspond to chlorophylls and red color correspond to astaxanthin.

1.3.2. Biochemical composition of *H. pluvialis*

H. pluvialis composition changes according to the cell stage, vegetative or green and induction or red stage. In green stage, protein content is higher than in red stage (Table 1.3) (Kobayashi *et al*., 1997a; Lorenz, 1999); the lipid content is divided in three types, the phospholipids, which are constant in both stages, neutral lipids and glycolipids that increase from green stage to red stage, and whose values will depend on the stress conditions and the used strain. In red stage, it is known that astaxanthin accumulation increases and there is an increase in the triacylglycerol (TAG) contents (Damiani *et al*., 2010; Saha *et al*., 2013; Zhekisheva *et al*., 2002). When exposed to stress, cells start to produce carbohydrates rather than fatty acids, however, with the continuous exposure to stress, carbohydrates are converted to fatty acids (Recht *et al*., 2012). Besides, secondary carotenoids are synthesized after exposure to environmental stress, in red stage. Primary carotenoids, such as chlorophyll, are replaced by the secondary carotenoid, mainly astaxanthin (Grewe and Griehl, 2008). Degradation of chloroplast coincides with the triacylglycerol (TAG) accumulation, while reducing membrane glycerolipids, especially those glycolipids making up the photosynthetic complexes and chloroplast membrane matrix (Gwak *et al*., 2014).

Table 1.3 – Composition of *H. pluvialis* biomass in green and red cultivation stages. n.d.: no data. Adapted from Shah *et al*., 2016.

Composition content (% of DW)	Green stage	Red stage
Proteins	29-45	17-25
Lipids (% of total)	20-25	32-37
Carbohydrates	15-17	36-40
Carotenoids (% of total)	0.5	2-5
β-carotene	16.7	1,0
Lutein	56.3	0,5
Zeaxanthin	6.3	n.d.
Astaxanthin (including esters)	n.d.	81.2
Canthaxanthin	n.d.	5.1
Chlorophylls	1.5-2	0

1.3.3. Astaxanthin biosynthesis in *H. pluvialis*

Under stress, *H. pluvialis* generate reactive oxygen species (ROS), such as H_2O_2, single oxygen ($^1O_2$), superoxide radicals (O_2^-), and hydroxide radicals ($^{\bullet}OH$). As a survival strategy to the unbalanced ROS generation, *H. pluvialis* induce astaxanthin accumulation, preventing damage on cellular components. Carotenoids act as accessory light-harvesting pigments, trapping light energy, protecting the photosystem from photo-oxidation by quenching ROS (Lemoine and Schoefs, 2010; Kobayashi *et al*., 1997b). Steinbrenner and Linden (2003), proven that general carotenoid biosynthesis is subject to photosynthetic redox control. The transfer of *H. pluvialis* cells from low-light conditions to moderate light intensity results in the reduction of the components of the photosynthetic electron transport including the plastoquinone pool. The plastoquinone pool acts as a redox sensor and its reduction subsequently leads to the transcriptional activation of genes involved in astaxanthin biosynthesis. Thus, redox regulation of genes involved in the synthesis of carotenoids is a prerequisite for the production of astaxanthin under stress conditions such as high light intensity, nutrient deprivation or ROS presence. When multiple stresses are applied simultaneously, different stress response mechanisms can be

activated, each one contributing to some extent to the overall cell protection and to improve carotenogenesis (Lemoine and Schoefs, 2010; Kobayashi *et al*., 1997b).

Biosynthesis of astaxanthin is a complex process that is highly up-regulated in conditions of stress and which coincides with the TAG accumulation, while reducing membrane glycerolipids, especially those glycolipids making up the photosynthetic complexes and chloroplast membrane matrix (Gwak *et al*., 2014). The biosynthesis of astaxanthin in *H. pluvialis* follows the general carotenoid pathway up to β-carotene formation. Astaxanthin synthesis might follow two main putative pathways (Figure 1.6): (i) the first pathway, starts with the β-carotene oxidation and have echinenone, canthaxanthin and adonirubin as intermediates; (ii) the second pathway, begin with the hydroxylation of β-carotene and have β-cryptoxanthin, zeaxanthin and adonixanthin as intermediates. These intermediates reveal the involvement of two enzymes β-carotene ketolase (BKT) and β-carotene hydroxylase (CrtR-b) in the conversion of β-carotene to astaxanthin. Although the specific steps of astaxanthin biosynthesis are carried out in the cytoplasm, the enzymes of the general carotenoid pathway appear to be localized in the chloroplast (Han *et al*., 2013; Lemoine and Schoefs, 2010; Shah *et al*., 2016; Vidhyavathi *et al*., 2008). Reported by Vidhyavathi *et al*. (2008) and Han *et al*. (2013), the preferential pathway for astaxanthin formation began with the oxidation of β-carotene. Vidhyavathi *et al*. (2008) demonstrated that the reduction in the BKT expression was reflected in the significant reduction of astaxanthin content. However, according to Gao *et al*. (2014) and Lemoine and Schoefs (2010), the two pathways can occur.

In *H. pluvialis* most of astaxanthin molecules are accumulate in red stage cells as cytoplasmic lipid bodies. The majority of astaxanthin exists as fatty acid esters, usually mono- or diesters of palmitic (16:0), oleic (18:1), or linoleic (18:2; 18:3), behaving as stabilizers to maintain a high antioxidant ability. The esterification is required for the deposition within the non-polar matrix of lipid droplets (Han *et al*., 2013; Lemoine and Schoefs, 2010; Shah *et al*., 2016; Vidhyavathi *et al*., 2008).

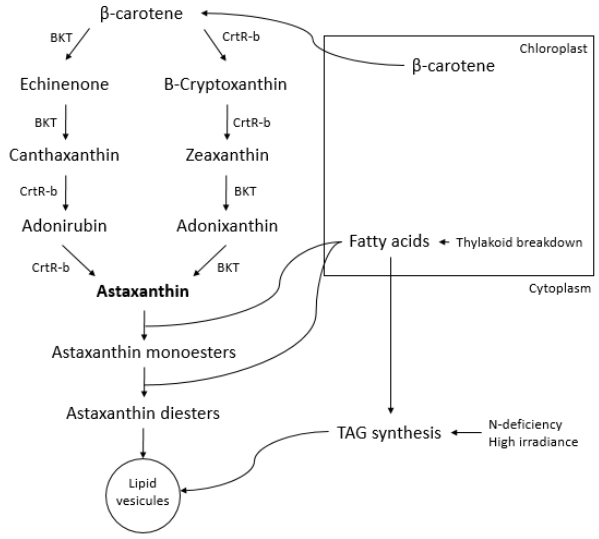

Figure 1.6 – Pathway of astaxanthin biosynthesis in *H. pluvialis*. Enzyme abbreviations are as follows: BKT, β-carotene ketolase; CrtR-b, β-carotene 3,3′-hydroxylase. Adapted from Lemoine and Schoefs, 2010, Gwak *et al*., 2014 and Han *et al*., 2013.

1.3.4. *H. pluvialis* growth and astaxanthin accumulation requirements

Due to specificity of *H. pluvialis* strains, optimization of cultivation parameters is necessary to achieve high biomass productivity and successful astaxanthin accumulation (Domínguez-Bocanegra *et al*., 2004; Fábregas *et al*., 2000; Lu *et al*., 2010; Suyono *et al*., 2015). Conditions for vegetative growth of the

green microalgae *H. pluvialis* comprise a large number of parameters. The effects of light intensity, inoculum concentration, nutrient saturation, carbon dioxide concentrations, strain used, among others, must be properly combined to achieve the successful production of microalgae, maintaining the culture with high astaxanthin productivity (Aflabo *et al*., 2007; Domínguez-Bocanegra *et al*., 2004; Fábregas *et al*., 2001; García-Malea *et al*., 2006; Sarada *et al*., 2002a).

Environmental factors are essential for *H. pluvialis* growth (green cells), such as: (i) temperature, about 20 to 28 °C (Wan *et al*., 2014); (ii) pH, between 7 and 8 (Borowitzka *et al*., 1991; Sarada *et al*., 2002b) since the intracellular microalgae pH is around 7; (iii) light intensity, ranging from 20 to 177 $\mu mol.m^{-2}.s^{-1}$ under continuous illumination or light–dark cycles (Boussiba, 2000; Domínguez-Bocanegra *et al*., 2004) have revealed themselves as crucial for microalgae development. The nutrients are one of the main factors that regulate morphological and physiological cellular responses of the microalgae, due to the impact on biochemical reactions, being the most important factor for the growth rate, composition, and high-value added products biosynthesis. The most important macronutrients for microalgae biomass production are carbon, nitrogen, phosphorus and sulfur.

These parameters are also adequate for induction stage when conjugated with stress factors (*e.g*. nutrient starvation and salinity) (Figure 1.7). Carotenogenesis may be fostered by low light intensities, 100 - 150 $\mu mol.m^{-2}.s^{-1}$ (Zhang *et al*., 2014), or by higher intensities that accelerate astaxanthin biosynthesis. An excess of light radiation (> 400 $\mu mol.m^{-2}.s^{-1}$) can be dangerous for microalgae viability due to ROS causing photoinhibition. However, the irradiation may become more efficient when conjugated with other stress factor, *e.g.* nutrient starvation, salt stress (Aflabo *et al*., 2007), addition of ethanol (Wen *et al*., 2015), hormones (Lu *et al*., 2010), fulvic acid (Zhao *et al*., 2015), nuclear radiation (Cheng *et al*., 2016) and many others factors that can be add to induce carotenogenesis in *H. pluvialis* (Forján *et al*., 2014; Sarada *et al*., 2002a; Su *et al*., 2014; Zhang *et al*., 2014).

In *H. pluvialis*, saline stress has been studied suggesting that it can replace light stress to induce carotenoid production; however, in several cases the microalgae growth decreased as NaCl concentration increased (Figure 1.7) (Benavente-Valdés *et al*., 2016). The effect of saline stress is largely studied by different autores (Aflabo *et al*., 2007; Boussiba and Vonshak, 1991; Borowitzka *et al*., 1991), although the optimal NaCl concentration to induce astaxanthin accumulation varies. However, is known that high NaCl concentration causes an increase in carotenoid content per cell (Tam *el al*., 2012). In conclusion, *H. pluvialis* can respond to various stress conditions in different ways. Whereas high light intensity leads to a transient response and to moderate accumulation of astaxanthin, the combination of various stress conditions such as high light intensity and salt stress is obligatory for encystment and the strong up-regulation of carotenoid genes (Steinbrenner and Linden, 2001).

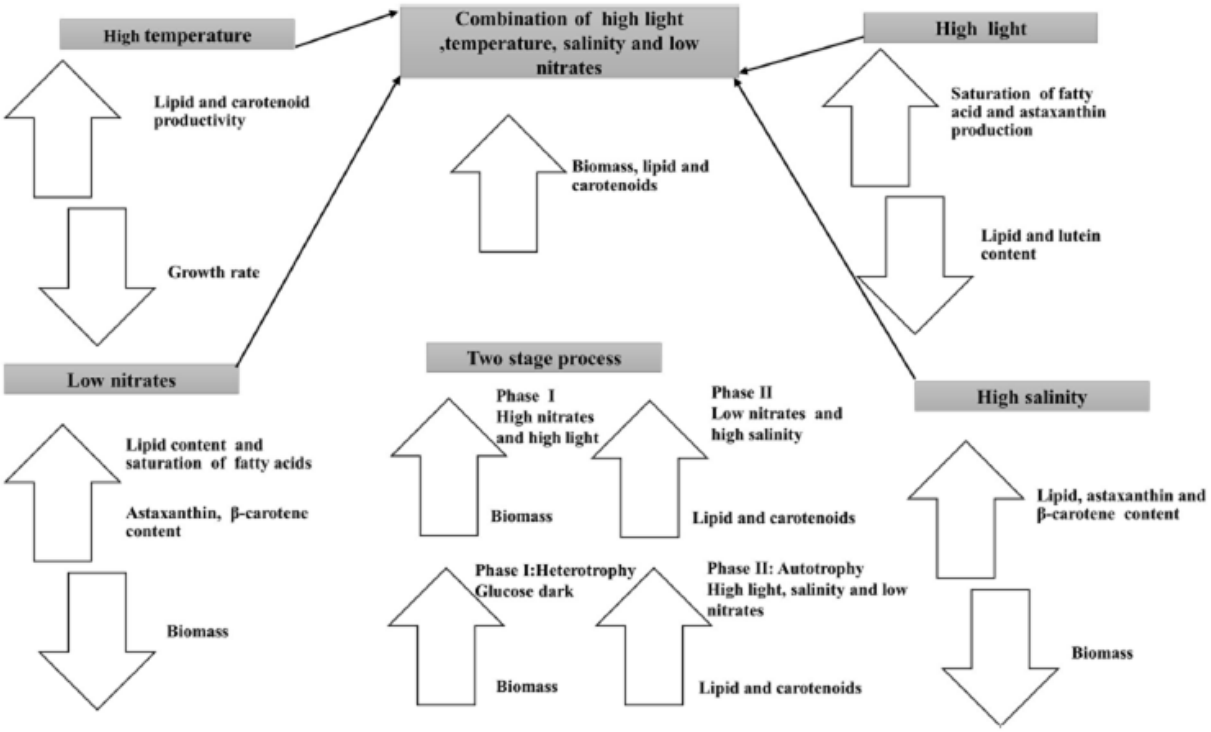

Figure 1.7 – Schematic diagram showing impact of environmental and nutrient factors on lipid and carotenoid production. Extracted from Minhas *et al*., 2016.

1.3.5. Large scale production of *H. pluvialis*

H. pluvialis is capable of growing in photoautotrophic (Aflalo *et al*., 2007), heterotrophic (Zhang *et al*., 2016), or mixotrophic growth (Kobayashi *et al*., 1992) conditions, indoors, in open raceway ponds or closed photobioreactors, in batch, in fed batch, or in continuous modes (Figure 1.8). As the optimal culture conditions for the production of biomass and accumulation of astaxanthin are not the same, two different strategies can be adopted in the production of *H. pluvialis*. One stage cultivation (Der Rio *et al*., 2007) that consists in continuous cultivation of *H. pluvialis* under moderate nitrogen limitation and specific average irradiance, resulting in simultaneous cell growth and astaxanthin accumulation; two-step cultivation (Fábregas *et al*., 2001) where the first stage aims to promote green vegetative growth under favorable culture conditions and in a second stage the cultures are submitted to stress factors in order to stimulate the transition to the aplanospore stage and the accumulation of astaxanthin. Nowadays, *H. pluvialis* is produced in two-stages, the most recent advances in cultivation for astaxanthin production include a two-stage mixotrophic culture system (Park *et al*., 2014) and attached cultivation system using the immobilized biofilm (Zang *et al*., 2014). Furthermore, each stage can be optimized for biomass growth and astaxanthin accumulation by adjusting independently the respective ratio of effective irradiance to cell density (Aflalo *et al*., 2007).

Li *et al*. (2011) estimated the production cost of astaxanthin, by his conceptually designed facility, to be \$718/*kg* astaxanthin or about \$18/*kg* biomass with 2.5 % astaxanthin. However, the cost is lower than the current industrial operations and is even lower than that of synthetic astaxanthin. The cost might even be able to be further reduced with the advances of technologies and optimization of processes. (Goswami *et al*., 2010; Lemoine and Schoefs, 2010; Li *et al*., 2011; Shah *et al*., 2016).

Technological advances are rapidly occurring in the microalgae-related industries. Top five leader commercial companies of *H. pluvialis* are: Cyanotech Corporation, USA; Mera Pharmaceutigals Inc., USA; Stazen Inc., USA; Valensa International, USA; Algatechnologies Ltd., Israel (Shah *et al*., 2016).

Figure 1.8 – Two examples of cultivation systems used at industrial scale. Culture ponds (500 000 liters) at Cyanotech Corporation (HI, USA) (left image); *H. pluvialis* production in photobioreator at A4F (right image).

1.3.6. Challenges for the improvement of *H. pluvialis*

There are many challenges and problems in the development of large-scale production of *H. pluvialis*. As an example, a challenging task with *H. pluvialis* is its outdoor cultivation which involves curtailment of contamination (mainly by fungi *Paraphysoderma sedebokerense* (Strittmatter *et al*., 2015)) and control of environmental conditions such as light and temperature. Since it grows at neutral pH, contamination by bacteria, fungi and protozoa, is the main problem.

However, improvement of astaxanthin production yield must not be confined to optimization of culture conditions and systems of production. Mutagenesis and selection of mutants can be used as an approach to increase strain performance. Mutants can be obtained by physical mutagens such as ultraviolet radiation (UV) or X-rays and chemical mutagens such as ethyl methanesulphonate (EMS) or N-methyl-N-nitro-N-nitrosoguanidine (NTG) for enhancing the production of astaxanthin (Chen *et al*., 2003; Kamath *et al*., 2008; Tjahjono *et al*.,1994; Tripathi *et al*., 2001). UV induced random mutagenesis has the advantage of not being classified as a genetically modified method. However, genetic engineering of microalgae has been applied for more competitive pigment production (Forján *et al*., 2015; Sharon-Gojman *et al*., 2015).

Despite those innovative techniques, another approach for strain improvement, is based on the overproducers isolation by performing cell sorting coupled with flow cytometry (Doan and Obbard, 2012; Terashima *et al*., 2015). This methodology allows a characterization at unicellular level by evaluation near real-time of the physiological and metabolic states of cells, and is useful for the evaluation, control and optimization of bioprocesses. Flow cytometry associated with a cell sorting device, had shown significant potential in isolation of microalgae (Pereira *et al*., 2011; Hyka *et al*., 2013). Cell sorting had been applied to improve microalgae strains for lipid increase or for acquisition of axenic cultures (Cabanelas *et al*., 2015; Sensen *et al*., 1993; Terashima *et al*., 2015; Wahby *et al*., 2014; Xie *et al*., 2014). Although the flow cytometer is an expensive equipment, this technique presents many advantages, such as rapid, accurate, precise and real time acquisition of data, allowing cell enumeration, viability and fluorescence measurements.

2 – OBJECTIVES

As already explained, among the important microalgae, *H. pluvialis* is the richest source of natural astaxanthin, which has important applications in the nutraceuticals, cosmetics, food and aquaculture industries. There are many challenges and problems for the development of large-scale production of biomass and astaxanthin from *H. pluvialis*.

The work performed for this thesis had as the main objective to improve *H. pluvialis* cultures to produce astaxanthin. For this purpose, seven *H. pluvialis* strains were screened and a characterization of microalgae was conducted throughout the cultivation process. This integrative characterization focused on the evaluation of: (i) the growth rate and biomass productivity during the green vegetative stage growth; (ii) astaxanthin accumulation throughout the induction stage under stress conditions (nutrient starvation and high light intensity) and under additional salinity stress. The parameters intended to be analyzed were: cell counting, dry weight and pigment analysis. The goal of the screening was to select strains with improved features or astaxanthin overproducers.

The fluorescence being derived from chlorophyll (autofluorescence) is a unique biomarker for photosynthetic organisms and enables setting a flow cytometric trigger for the separation of microalgae from other particles and microorganisms. To complement the screening, was also monitored by flow cytometry, the evolution of cytological and physiological properties (cell size, cell complexity and fluorescence) being derived from pigments (autofluorescence) of the *H. pluvialis* strains, at the beginning of the cultures, when each strain was separately inoculated into the growth media, and along the induction stage.

After the selection of strains with improved features, two other strategies were used for improvement of astaxanthin production capacity: UV induced random mutagenesis and separation of cells that differ in astaxanthin content, by flow cytometry equipped with a sorting device.

3 – MATERIALS & METHODS

3.1. MICROORGANISM

For this thesis, seven strains of *H. pluvialis* from A4F – Algafuel, S.A. culture collection were analyzed. The code names for the strains used are HP_01 to HP_07.

3.2. CULTIVATION CONDITIONS

H. pluvialis cultivation for astaxanthin production was performed using a 3-steps strategy. Each strain was prepared in duplicate and two independent repetitions were carried out, using for each one, different initial inoculum. The assays comprised three stages, started with a green vegetative growth stage, followed by an astaxanthin accumulation induction stage and ended with a stage of an additional salinity stress, whose aim was to promote further the astaxanthin accumulation. For production of *H. pluvialis*, some optimizations were adopted in order to grow them in the best conditions (Table 3.1).

In Table 3.1 are shown the cultivation conditions, during each stage. Bubble columns (700 mL) were used to grow all strains under the same conditions. The green vegetative growth stage lasted seven days, at about 90 $\mu mol.m^{-2}.s^{-1}$ of light intensity, and complete growth media was provided with all nutrients required. In the first stage of the assay, cultures were in optimal conditions for growth, sampling and cell counts were performed daily, while the determination of the dry weight and pigment analyses were carried out only at the beginning and end of this stage.

Induction stage lasted 17 days at 150 $\mu mol.m^{-2}.s^{-1}$ of light intensity, and no nutrients were supplied. The stresses applied were light intensity, which was controlled by the distance from the bubble columns to the cool white fluorescent lamps, and nutrient starvation. At this stage, samples were collected three times a week. Analytical methods, such as cell counting, flow cytometry, dry weight and pigment analyses, were realized whenever the sample collection was performed. At the end of induction stage, flow cytometry and cell sorting was applied to the strains of *H. pluvialis* that were selected by previous screening for having improved features.

In the additional stress, last stage, the culture salinity was adjusted to 10 $g.L^{-1}$ of NaCl. Once again, sample collection was performed three times a week and the same analytical methods were carried out.

Table 3.1 – Cultivation conditions for the 3 phases of the assay.

	Growth Stage	Induction Stage	Induction stage plus salinity
System	Bubble column	Bubble column	Bubble column
Volume	700 mL	700 mL	700 mL
Initial concentration	0.2 $g.L^{-1}$	0.6 $g.L^{-1}$	-
Light intensity	≈90 $\mu mol.m^{-2}.s^{-1}$	≈150 $\mu molm^{-2}.s^{-1}$	≈150 $\mu mol.m^{-2}.s^{-1}$
Temperature/ Pressure	25 ± 1 ºC/ environmental	25 ± 1 ºC/ environmental	25 ± 1 ºC/ environmental
Photoperiod	24 h light	24 h light	24 h light
Carbon source	Air + 0.5 % CO_2	Air + 0.5 % CO_2	Air + 0.5 % CO_2
Salinity	0 $g.L^{-1}$	0 $g.L^{-1}$	10 $g.L^{-1}$
Growth medium	autoclaved tap water	autoclaved tap water	autoclaved tap water + NaCl
Nutrient medium	Nutrient medium developed in A4F*	No nutrient addition	No nutrient addition
Sample collection	Daily (at 9 a.m.)	3x week (at 9 a.m.)	3x week (at 9 a.m.)
Duration	7 Days	17 Days	6 Days

*Based on the experience, A4F has developed a nutritive media for laboratory cultivation of several microalgae strains. This nutritive media is composed by the macro-nutrients – nitrogen, phosphorous and iron; micro-nutrients – *e.g.* magnesium, zinc, etc., and is supplemented with vitamins and further sterilized (Fábregas *et al*., 2000).

3.3. ANALYTICAL METHODS

3.3.1. Microscopy observation

The cells were observed using a BX53 microscope (Olympus, Tokyo, Japan) whenever the sample collection was realized. This is a quick method that allows monitoring the evolution of the cultures, though the physiological cell state analysis, cell division, and the detection of contaminations, clumps and debris.

To follow the life cycle of *H. pluvialis*, the Microscope Leica DM5500B was used. The filters used to observe the samples are present in Table 3.2.

Table 3.2 – Emission and excitation of the filter, respectively. BP – band pass; HP – high quality.

	Emission	Excitation
Astaxanthin Detection	BP 610/75	HQ 545/12
Chlorophyll Detection	BP 700/38	BP 630/30

3.3.2. Cell Counting

The microalgae growth was determined by cell counting (Microscope Olympus BX53) with a 0.1 mm^3 Neubauer chamber (Marienfeld – Laboratory Glassware) and each sample was counted in triplicate.

3.3.3. Cell Counting & viability analysis

Muse® cell analyzer (Merck-Millipore, USA) is an equipment that enables precise and accurate counts and viability measurements at a single cell level in real time. For cell counting, 500 µL sample was read

in triplicate. Using a multiparametric detection of individual cell via microcapillary flow technology, the system enables highly sensitive and rapid detection of cellular samples using minimal cell numbers. The flow cell of the instrument is engineered for the acquisition of cells from 2-60 µm in diameter and to accurately detect the fluorescence emitted by cells when excited by a green laser (532 nm).

Muse® uses fluorescent reagents and detection to measure three parameters, cell size (forward scatter) and 2 colors (detected in the red and/or yellow channels). Propidium iodide (PI) (AGROS organics) is a fluorescent dye, which gets inside the cells that have cell membrane compromised, staining the nonviable cells, binding to nucleic acid inside it. When the cultures are submitted to a stress, cells can be disrupted, losing the ability to function normally. Because of this different behavior of the damage cells, was used PI at a final concentration of 10 % (v/v) to quantify the nonviable cells. The assay utilizes a proprietary mix of one DNA intercalating fluorescent dyes and chlorophyll fluorescence. This combination allows for the discrimination of nucleated cells from those without a nucleus or debris, and live cells from dead or dying resulting in both accurate cell concentration and viability results.

3.3.4. Dry weight (DW)

For this method, the moisture analyzer (MS 70 – AND) was used to heat the sample at 180ºC with halogen lamp and measure the DW in g/L. The samples of the cultures were filtered, using 1.2 µm diameter pore (Microfibre Filter Paper), in pre-weighed filters and then dried in the moisture analyzer. The DW is calculated using the following equation 3.1, where mI and mF correspond to initial mass, before filtration, and final mass after filtration (g), respectively and Vol to volume (L).

$$DW\ (g.L^{-1}) = \frac{mF - mI}{Vol}$$

Equation 3.1 – Determination of dry weight.

3.3.5. Pigments analysis

Chlorophylls and carotenoids contents were determined by total wavelength spectrophotometric scan (Genesys 10S UV-Vis (± 0.005 AU) – Thermo Scientific, US) of the pigment solution obtained from biomass samples by extraction with bead beating and acetone. Each sample was read in duplicate in quartz cuvettes, with 1 cm of path, against an acetone blank.

A mathematical algorithm to determine and quantify the pigments, based on Beer-Lambert law was developed, by A4F, as a fast and inexpensive way of predicting chlorophylls and carotenoids concentration from microalgae cultures. The Beer-Lambert law is used to convert every absorption value in the spectrum into a concentration of pure pigment (Equation 3.2).

$$A(\lambda)=c\_1\ \varepsilon\_1\ (\lambda)+c\_2\ \varepsilon\_2\ (\lambda)+\cdots+c\_n\ \varepsilon\_n\ (\lambda)$$

Equation 3.2 – Beer-Lambert law.

The mathematical algorithm was applied to the full spectra obtained and the concentration of pigments determined (Costa *et al*., 2008). As bac*kg*round information, it is necessary to know the pigments present in the extract under analysis, or at least the more relevant ones, that are going to set the main tendencies of the spectrum. It is also necessary to have the UV/vis spectrum of each pure pigment extract and the molar absorbance as well, in order to combine all the spectra in one to reach. The results can be expressed in $mg.g^{-1}$ DW or in $mg.L^{-1}$.

3.3.6. Cultures growth

The specific growth rate, μ (day^{-1}) (Equation 3.3), was based on cell counting (section 3.3.2.). Biomass productivity ($g.L^{-1}.day^{-1}$) were determined using Equation 3.4, based on DW (section 3.3.4) and astaxanthin productivity (mg.g $DW.day^{-1}$ or $mg.L^{-1}.day^{-1}$) were determined using Equation 3.5, based on pigment analysis (section 3.3.5).

$$\mu\ (day^{-1}) = \frac{Ln(C_2) - Ln(C_1)}{t_2 - t_1}$$

Equation 3.3 – Determination of growth rate.

$$Biomass\ productivity\ (g.L^{-1}.day^{-1}) = \frac{DW_2 - DW_1}{t_2 - t_1}$$

Equation 3.4 – Determination of volumetric biomass productivity.

$$Astaxanthin\ productivity\ (mg.g\ DW.day^{-1}\ or\ mg.L^{-1}.day^{-1}) = \frac{AC_2 - AC_1}{t_2 - t_1}$$

Equation 3.5 – Determination of astaxanthin productivity.

Where C_1 and C_2 correspond to initial and final cell concentration ($cells.mL^{-1}$), respectively, t_1 and t_2 correspond to initial and final culture time points (days) per identified growth period, respectively. DW_1 and DW_2 correspond to initial and final dry weight ($g.L^{-1}.day^{-1}$). AC_1 and AC_2 correspond to the initial and final astaxanthin content ($mg.g^{-1}$ DW or in $mg.L^{-1}$).

3.3.7. Nitrate determination

First, the culture samples were pelleting by centrifugation at 3500 rpm for 10 min in centrifuge Hermle Z 400 K. The supernatant obtained was diluted using distilled water and HCl (1 M) was added at a final concentration of 3 % (v/v) to prevent interferences from other absorbing compounds (such as hydroxide or carbonate anions). Each sample was read in duplicate in quartz cuvettes, with 1 cm of path, against distilled water.

The concentration of nitrate in the cultures medium was determined by ultraviolet spectrophotometry, measuring the sample absorbance at 220 and 275 nm (Genesys 10S UV-Vis (± 0,005 AU) – Thermo Scientific, US), and applying the Equation 3.6, where Abs NO^{3-} correspond to total absorbance of nitrates; Abs (220 nm), absorbance of nitrates at λ=220 nm and Abs (275 nm), absorbance of nitrates at λ=275 nm. Measurement of the UV absorption at 220 nm allows a rapid determination of nitrate, however, dissolved organic matter can also absorb at this wavelength. Therefore, using a second absorption value at 275 nm, a correction was made; at this wavelength, nitrates do not absorb, but the dissolved organics compounds absorb. The calibration of nitrates concentration was previous realized using standard solutions.

$$Abs\ NO_3^-(mM) = Abs\ (220\ nm) - 2\ x\ Abs\ (275\ nm)$$

Equation 3.6 – Correction of determination of nitrate ion concentration.

3.3.8. Statistical analysis

Statistical analysis of some data was analyzed with IBM® SPSS® Statistics version 23 by performing one-way analysis of variance (ANOVA) and, when differences observed were significant, the means were compared by multiple-range Bonferroni test. *P*-values equal or inferior to 0.05 were considered statistically significant.

3.4. FLOW CYTOMETRY AND CELL SORTING

3.4.1. Basic Principles of Flow Cytometry

Flow cytometry (FC) is a powerful technique for multiparametric analysis of physiological state of individual cells, already well established in environmental studies of microalgae. Improvements and technical advances in recent years, made this technology be recognized as a first choice in analysis in biotechnology (Hyka *et al*., 2012). FC enables single cells with different features to be counted, analyzed and sorted on the basis of scattered and fluorescent light signals. A special characteristic of microalgae is the presence of photosynthetic pigments that exhibit strong autofluorescence. A flow cytometer is composed by three main systems properly integrated, fluidics, optics and electronics (Table 3.3).

Table 3.3 – Basic components of Flow Cytometry.

Component	Function
Fluidics system	Responsible for the hydrodynamic focusing brings the particles of interest to the interrogation point.
Optics systems	Composed of light sources, lenses, optical filters and light detectors that all together make possible the detection of signals.
Electronics systems	Responsible for the transformation of the information detected by light detectors into an electric signal and later into a digital format.

Cells are conducted within a hydrodynamically focused fluid stream, passing through an excitation source (usually a laser beam) and the information/data of each single cell light scattering and/or fluorescence emission (the latter typically when fluorescent dyes are applied) is captured and recorded. This data is then converted into a digital format that ultimately is correlated to structural and/or functional cell parameters.

3.4.2. The Instrument

Flow cytometry analysis was performed using a CyFlow Space – Partec flow cytometer equipped with two excitation lasers, one of 488 nm (blue laser) and the other of 635 nm (red laser); light scattering occurs when a particle or a cell deflects incident laser light. The extent to which this occurs depends on the physical properties of a cell, namely its size and internal complexity. Factors that affect light scattering are the cell membrane, the nucleus and any granular material inside the cell. Cell shape and surface topography also contribute to the total light scatter. The forward scatter light (FSC - light scatter at low angles) provides information on cell size, although there is no direct correlation between size and FSC. Light scattered in an orthogonal direction can also be collected by a different detector (a side scatter or SSC detector), which provides information about granularity and cell morphology.

The flow cytometer is still equipped with four optical filters and detectors: 536/40 nm (FL1 green fluorescence), 575 nm (FL2 orange fluorescence), 610/30 nm (FL3 red fluorescence) and 675 nm (FL4 far red fluorescence) (Figure 3.1). Acquired data by FC is usually represented into monoparametric histograms (frequency distributions), biparametric histograms and dot plots. While one parameter histograms represent the number of cells or particles (y-axis) *versus* the scattering or fluorescence

intensity (x-axis), biparametric histograms are suitable to establish correlations between two parameters (Díaz *et al*., 2010).

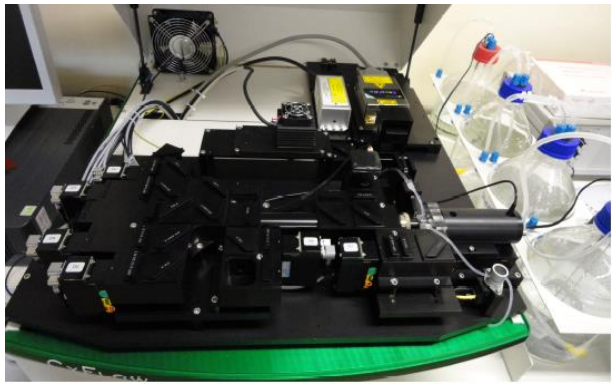

Figure 3.1 – Flow cytometry CyFlow Space – Partec.

For analysis of *H. pluvialis* subpopulations, chlorophyll rich and astaxanthin rich cells, flow cytometry signals gathered in FL4 and FL2 detectors correspond to red fluorescence emitted by chlorophylls and yellow fluorescence emitted by astaxanthin, respectively, after being excited at 488 nm. Also, to analize the viability of *H. pluvialis*, was applied the slow-response potential-sensitive probe [$DiBAC_4(3)$], with an incubation at room temperature in darkness for 30 min before submitted to FC. $DiBAC_4(3)$ can enter depolarized cells where it binds to intracellular proteins or membrane and exhibits enhanced fluorescence and a red spectral shift. Increased depolarization results in additional influx of the anionic dye and an increase in fluorescence. Conversely, hyperpolarization is indicated by a decrease in fluorescence. This bis-oxonal has an excitation maxima of 490 nm, emission maxima of 516 nm and detectable with FC as green fluorescence (536/40 nm).

At acquirements, gains were set to a specific and adequate value kept for all analysis. Logarithmic amplification was chosen and, as microalgae possess fluorescing endogenous pigments (chlorophylls and carotenoids), which are detectable with FC as red and orange autofluorescence, the trigger was set on red fluorescence (FL4) to exclude any cell debris or bacteria. The flow rate was kept at lowest setting (between 1000 and 2000 events per second), to ensure accuracy and precision. A fixed number of events (25 000) was set for each analysis so samples could be compared.

CyFlow Space – Partec cytometer allows the concentrations determination of any cell subpopulation of interest using True Volumetric Absolute Counting (TVAC). This method is based on the analysis of a fixed volume as defined by the distance between two platinum electrodes reaching into the sample tube with a given diameter.

Data was explored and analyzed by Operating Software FloMax® (version 2.7). The histograms and pseudocolor plots were extracted from FlowJo Software (version 10.0.7).

3.4.3. Cell Sorting

Partec CyFlow Space is able to physically separate (sort) cell subsets based on their optical characteristics, permitting further studies to be conducted. The sorting flow cell is a closed sorting system which has a y-shaped capillary channel, divided into the waste and sort channels. The operation of this device is based on a piezo crystal, located in the waste channel, which generates high speed pressure waves while cells are detected in the software sort regions. This pressure wave deflects those cells out of the laminar sample flow into the sort channel outlet. Sample collected enters the sorted

cuvette in a laminar stream, incorporated in the sheath. The piezo action does not disturb the laminar flow, due to the settings well establish before, so the pressure wave only will act on the pretended cells.

3.4.4. Defined settings to perform cell sorting

For performing cell sorting, three parameters had to be defined, trigger delay, pulse width and voltage. After different optimization experiments, the most appropriate parameters were defined (Table 3.4).

Table 3.4 – Defined parameters to perform cell sorting.

Trigger Delay	Pulse Width	Volts
0	10	0.65

3.5. MUTAGENESIS BY ULTRAVIOLET LIGHT

After the characterization of the seven strains, random mutagenesis using UV-C (254 nm) has been applied to improve *H. pluvialis* strains for astaxanthin accumulation (Tripathi *et al*., 2001; Vigeolas *et al*., 2012). Mutants were produced by exposing the vegetative green cells, in logarithmic phase (growth conditions described in Table 3.1), to UV radiation at different time intervals.

3.5.1. Dose-response curve determination

Culture from *H. pluvialis* was collected into a 50 mL quartz flask. The quartz flask was placed on top of the transilluminator UV light (254 nm, Transilluminator Benchtop 3UV^{TM}) during periods of 5 s, from 30 s until complete the 110 s of exposure (Figure 3.10), and agitating several times manually the samples. Between the expositions period, samples (2 mL) were taken into a sterile 24 well plate. This procedure was repeated three times. After complete the exposures the 24 well plates were kept at dark conditions overnight at 4ºC, to prevent photo reactivation. To determinate the dose-response curves, after overnight incubation, the samples collected were submitted to Muse® cell analyzer, using PI to stain the nonviable cells. The method is already described above (section 3.3.3.). For comparison and for each strain, samples of an unmutated cell culture were taken from a flask culture under logarithmic growth.

3.5.2. Mutants generation

H. pluvialis culture, previously collected to a 100 mL quartz flask, was exposure to 70 s of UV-C, 254 nm, on top of Transilluminator Benchtop 3UV^{TM}. The culture after exposure was transferred to a sterile 100 mL flask. This procedure was repeated three times. After complete the exposure the three flasks were kept overnight in the dark at 4ºC. After this period, was performed a cell counting on Muse® for assessing cell viability, using PI staining and it began then on scale-up regimen.

4 – RESULTS & DISCUSSION

4.1. THREE-STAGE CULTURES FOR ASTAXANTHIN PRODUCTION

The seven A4F *H. pluvialis* strains were cultured twice, and their characterization was carried out in order to select the best strains for astaxanthin production. Results presented here are from one assay since the same trend was observed in both assays.

The first cultivation step (green vegetative growth) started with all strains with an identical inoculum biomass of 0.2 $g.L^{-1}$ (Figure 4.1A), although differences have been observed in the initial cell density (Figure 4.2 (green bac*kg*round)). As it was expected, the growth of microalgae cultures was characterized by three distinct phases: (i) the first day after inoculation, the strains were in the latent phase with a continuous low growth rate, which correspond to a period of cells adaptation to the new operating conditions; (ii) during the 2^{nd} to 4^{th} days they were in the logarithmic phase with high cell activity; (iii) since the 4^{th} day after inoculation the strains reached the stationary phase where cell density remained constant (Figure 4.2 (green bac*kg*round)). The highest value of cell density ($1.79x10^6$ $cell.mL^{-1}$) was obtained for HP_03 strain, reached in the last day of exponential growth phase, and similar cell density was observed in HP_05 ($1.73.x10^6$ $cell.mL^{-1}$), followed by HP_07 ($1.67x10^6$ $cell.mL^{-1}$), HP_02 ($1.57x10^6$ $cell.mL^{-1}$) and HP_04 ($1.09x10^6$ $cell.mL^{-1}$). HP_01 and HP_06 showed the lowest values, reaching only $2.67x10^5$ and $2.36x10^5$ $cell.mL^{-1}$, respectively.

Overall, all strains had quite comparable growth behaviors. However, several factors may contribute to the observed differences in maximum cell density achieved in the stationary phase; some of these differences may be due to the natural physiological variability of the strains, namely the requirement of specific nutrients and cell size. Cultures were maintained during seven days in a batch regime, supplemented with A4F nutrient medium. The medium used in this work is similar to optimal *Haematococcus* media (OHM) (Fábregas *et al*., 2000). However, Fábregas *et al*. (2000) obtained a maximum cell density of 5.72×10^5 $cell.mL^{-1}$ in a semi-continuous regime with a daily renewal of 10 % of the volume of the culture, during eight days. Despite differences observed between strains, A4F medium have proven to be a promising alternative of OHM, since in a shorter period (seven days), cell density exceeded the described value in the literature, $1.79x10^6$ $cell.mL^{-1}$ in HP_03. Fábregas *et al*., 1998, obtained $6.25x10^5$ $cell.mL^{-1}$ in a batch culture after fourteen days, with a previous optimized OHM. In other reports, different values, such as $1x10^6$ $cell.mL^{-1}$ (Tocquin *et al*., 2011), $1.33x10^5$ $cell.mL^{-1}$ and $1.08x10^5$ $cells.mL^{-1}$ (Sipaúba-Tavares *et al*., 2013) and 8.00×10^5 $cell.mL^{-1}$ (Kaewpintong *et al*., 2007) were obtained in different nutrient media and cultivation conditions. The light intensity and its regime, the culture medium, cultivation systems and volumes of the cultures, influence the maximum of cell density. During batch cultivations under constant light intensity, the cells may undergo photo-inhibition at early growth stage and light limitation at higher cell concentration leading to a linear growth phase. Thus, it is important to maintain the light conditions within an appropriate range during the entire cultivation period (Choi *et al*., 2003).

The induction stage for astaxanthin accumulation was initiated with a dilution of cultures to adjust the biomass concentration of the different strains to 0.6 $g.L^{-1}$. On the first day of induction, the nitrate concentration measured was 0 mM for all strains considered. However, as shown in Figure 4.1B, some cultures were reacting to the lack of nutrients before the induction and it was verified that they were already at this stage, due to the reduced quantity of nutrients provided in the last two days of growth

stage. Once again, differences in the initial cell density were observed (Figure 4.2 (red bac*kg*round)) due to their natural physiological variability. During exposure of the strains to the stress conditions, it was observed a general response pattern, manifested by the maintenance of cell density up to day 21 of the assay, followed by a decrease in the number of the cells in the last 3 days of the induction phase. It should be noteworthy, that the HP_07 seems to be the more resistant strain to stresses, as this strain was the only one to show an increase in cell concentration during the induction phase of astaxanthin accumulation (Figure 4.2 (red bac*kg*round)).

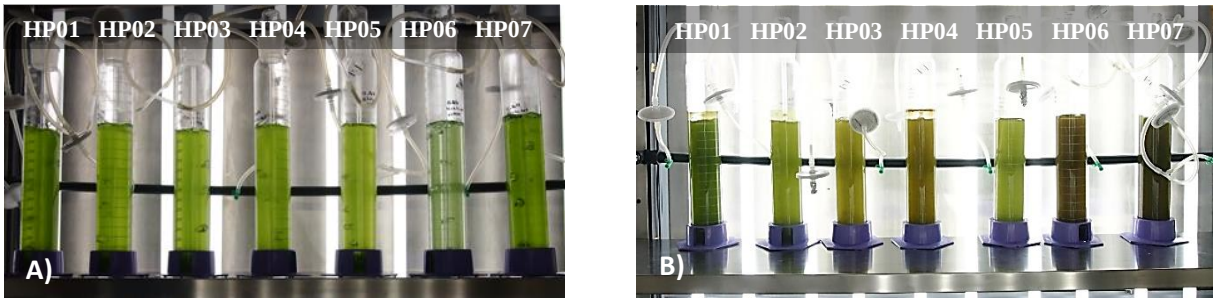

Figure 4.1 – Macroscopic evolution of the cultures during the assay. A) cultures after inoculation (to 0.2 $g.L^{-1}$), day 0 of vegetative stage and B) cultures after renewal (to 0.6 $g.L^{-1}$), day 0 of induction stage;

In the last additional stress phase, after further dilution and increased salinity of cultures, cell density remained stable in all cultures studied (Figure 4.2 (orange bac*kg*round)).

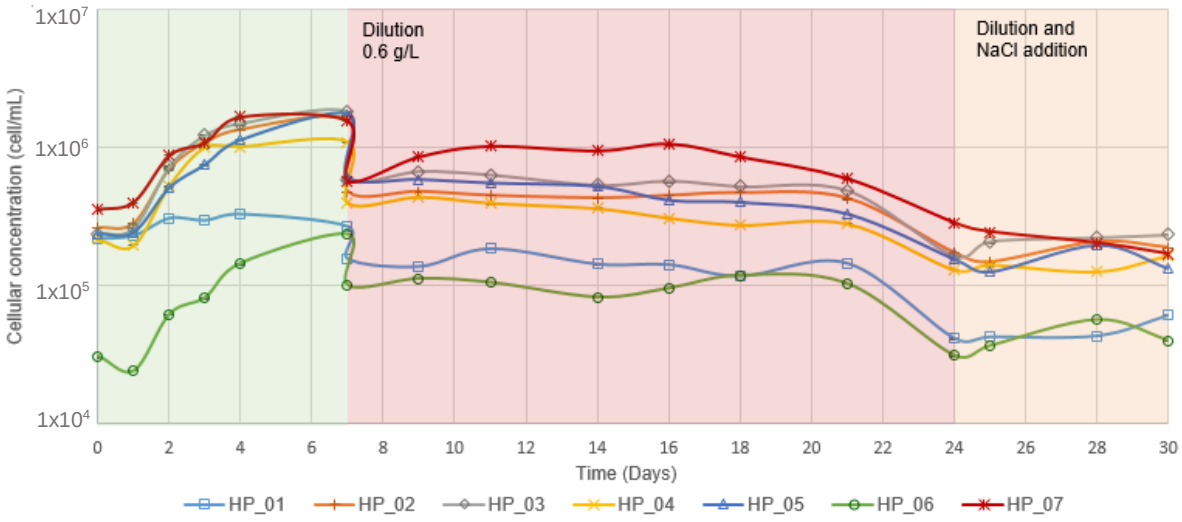

Figure 4.2 – Cultures evolution during the assay. Evolution of cellular concentration throughout the 30 days of assay; culture conditions corresponding to the three stages: green bac*kg*round indicates the vegetative stage and optimal conditions; red bac*kg*round indicates the induction stage, with nutrient starvation and high light intensity; orange bac*kg*round indicates the additional salinity stress. Error bars show the based on standard deviation among technical triplicates on Neubauer Chamber counting.

4.1.1. Characterization of Vegetative Growth Stage

The first stage, green vegetative growth phase, was performed to obtain a large quantity of green vegetative cells under the favorable culture conditions. The results are presented in the Figure 4.2 (green bac*kg*round). The analysis of results allows to highlight the different kinetics of HP_01 and HP_06 strains: although the initial inoculum was identical to that of most strains, HP_01 reached the lower cell density ($2.67x10^5$ $cell.mL^{-1}$) and showed the lowest growth rate (0.12 day^{-1}).

The results acquired showed that, in terms of growth rate, strain HP_03 (0.58 ± 0.00 day^{-1}), obtained the greater value, followed by HP_04 (0.55 ± 0.03 day^{-1}) and HP_02 (0.52 ± 0.01 day^{-1}). HP_01 (0.12 ± 0.01 day^{-1}) presented the lower growth rate (Figure 4.3). A constant growth rate can be maintained yielding high biomass productivity if previous parameters are kept at an optimum level, preventing carotenogenesis induction (Aflabo *et al*., 2007, Park *et al*., 2014). In the literature, different values of growth rates have been reported, possibly due to the heterogeneity of the cultivation conditions. Growth rates under autotrophic conditions range from 0.19 to 0.96 day^{-1} (Aflabo *et al*., 2007; García-Malea *et al*., 2006; Kaewpintong *et al*., 2007; Kobayashi *et al*., 1992); under heterotrophic and mixotrophic conditions growth rates of 0.22 day^{-1} and about 0.58 day^{-1} were respectively reported (Kobayashi *et al*., 1992). Taking in account the conditions set in the assays, the results obtained, presented in Figure 4.3, are consistent with the values reported in literature, except for HP_01 that presented the lowest result (0.12 ± 0.01 day^{-1}). This strain, in Figure 4.2 green bac*kg*round, did not present an increase in cell number, verified for as the rest of the strains tested.

Overall, the strains had quite comparable biomass productivity (g $DW.L^{-1}.day^{-1}$) during the seven days of the growth vegetative stage (Figure 4.3), except for HP_06 and HP_07 strains, which had the lowest productivity (0.15 ± 0.02 and 0.16 ± 0.02 g $DW.L^{-1}.day^{-1}$ respectively). The highest value, 0.27 ± 0.02 g $DW.L^{-1}.day^{-1}$, reached by HP_01 and HP_02 strains was lower than the values obtained by Aflabo *et al*. (2007) and Garcia-Malea *et al.* (2006) (up to 0.5 g $DW.L^{-1}.day^{-1}$). However, it is noted that the results were consistent with what has been observed by other authors under autotrophic conditions, 0.07 g $DW.L^{-1}.day^{-1}$ (Fabregas *et al*., 2001), heterotrophic conditions 0.17 g $DW.L^{-1}.day^{-1}$ (Hata *et al*., 2001) and mixotrophic conditions, 0.20 g $DW.L^{-1}.day^{-1}$ (Del Campo *et al*., 2004).

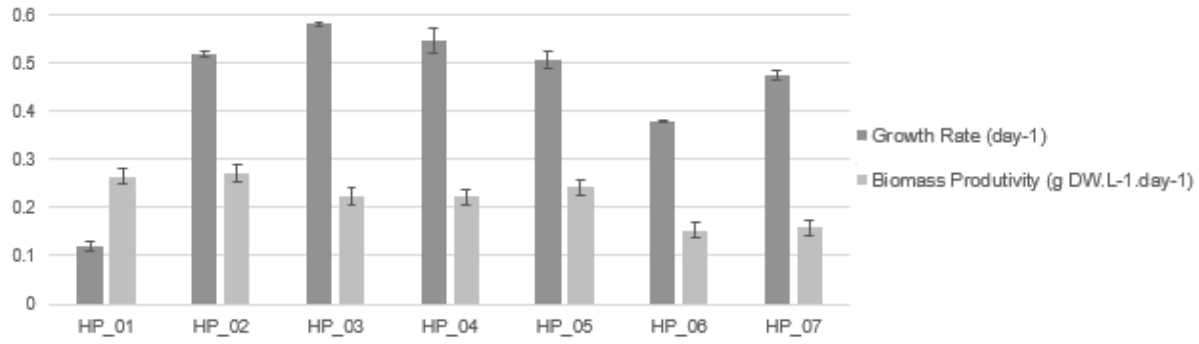

Figure 4.3 – Growth rate and biomass productivity in the vegetative stage. Errors bars were based on standard deviation from the technical triplicates on Neubauer chamber and from uncertainty of DW.

At the end of the vegetative growth phase, higher biomass productivity was expected, since growth rate was higher than the one reported in the literature. Different culture conditions (light intensity and nutrients availability), experimental designs and strains utilized are likely to explain the differences observed in the literature survey. However, productivity of vegetative cells of *H. pluvialis* are regulated by the average of irradiance, nutrients content of the medium, and to its sensitivity to changes on culture conditions (García-Malea *et al*., 2005). The effect of light intensity is dependent on the nutritional state of the culture, vegetative growth may be maintained at high light intensity if nutrients are available, avoiding carotenogenesis induction (Fábregas *et al*., 2000). The later the stationary phase was reached, the higher the biomass yield was at the end of cultivation. Also, differences between growth rate and biomass productivity were reflected in cell weight (Table 4.1).

When a culture has a greater proportion of palmelloid cells than flagellated cells, is indicative of adverse environmental conditions for rapid growth (González *et al*., 2009). Comparing HP_01, HP_02 and

HP_03 strains, it appears that, although HP_01 strain has shown a much lower growth rate in terms of cell number (approximately five times smaller), however, the biomass productivity was similar in the three strains. In the case of HP01 strain, the energy from substrate utilization seems to have been used to meet the maintenance requirements, reflected in an increase of biomass (Table 4.1).

During growth, there is normally an increase in cell mass, which is reflected in an increase in the number of cells. However, a direct general relationship between cell number and dry weight measurements cannot be established, due to the great variation of cell weight between different cell types, which can vary from 500 pg.cell^{-1} weight for flagellated cells, to 1000 pg.cell^{-1} for palmelloid cells and even 3000 pg.cell^{-1} for cysts (López *et al*., 2006). According to the results, HP_07 was the strain that showed the lowest dry weight (Table 4.1), a growth rate relatively high and low biomass productivity; however, it should be emphasized that this was the only strain retained flagellated cells throughout the vegetative growth phase. The HP_01 and HP_06 strains showed the highest increase in dry weight throughout the assay, having been detected a predominance of palmelloid cells in the cultures. In the remaining strains, the flagellated cells predominated in cultures and palmelloids cells were observed only at the end of the exponential phase.

Table 4.1 – Average of weight per cell. Measured at the beginning and at the end of the vegetative growth stage.

	HP_01	**HP_02**	**HP_03**	**HP_04**	**HP_05**	**HP_06**	**HP_07**
Initial pg.cell^{-1}	1066.48	960.72	837.28	961.33	949.94	4680.60	399.59
Final pg.cell^{-1}	5287.50	1336.16	984.20	1607.34	1096.81	5383.07	845.57

During the life cycle of the algae, green vegetative cells contain high levels of chlorophyll and protein. Predictably, under favorable conditions, *H. pluvialis* strains, presented a high content of chlorophylls (>25 mg.g^{-1} DW) and low content of carotenoids (<9 mg.g^{-1} DW). The maximum chlorophyll content was hit by HP_07 (34.90 ± 2.62 mg.g^{-1} DW), which also had the highest content of total carotenoids (8.44 ± 0.97 mg.g^{-1} DW) (Table 4.2). Overall, all strains showed an average chlorophyll content of 2.55 % (w/w) DW and an average carotenoids content of 0.84 % (w/w) DW. This values were in agreement with previously reported assays where green cells showed an average chlorophyll content of 2.4 ± 0.11 % (w/w) DW and an average primary carotenoid content of 0.48 ± 0.03 % (w/w) DW (Grewe and Grield, 2008).

Table 4.2 – Total of chlorophylls and carotenoids in the vegetative stage in the first day of growth stage. Total chlorophylls comprise chlorophyll a and b; Total carotenoids comprise astaxanthin, cantaxanthin, neoxanthin, violaxanthin, lutein, zeaxanthin and β-carotene. Error was based on standard deviation of technical triplicates from pigment analysis.

Vegetative stage	**Total Chlorophylls (mg.g^{-1} DW)**	**Total Carotenoids (mg.g^{-1} DW)**
HP_01	30.79 ± 4.24	6.22 ± 0.99
HP_02	31.15 ± 0.60	7.06 ± 0.13
HP_03	28.81 ± 0.84	6.48 ± 0.24
HP_04	25.51 ± 0.01	5.79 ± 0.04
HP_05	28.55 ± 0.46	6.75 ± 0.20
HP_06	30.29 ± 1.79	7.47 ± 0.16
HP_07	34.90 ± 2.62	8.44 ± 0.97

To summarize, the characterization of the all strains in terms of growth rate and biomass productivity allowed selecting, during the growth vegetative stage, HP_02, HP_03, HP_04 and HP_05 as the most promising strains. These results should be further supplemented with data obtained in the other stages of the assay.

4.1.2. Characterization of Induction Stage

It is reported in many studies that the accumulation of astaxanthin in *H. pluvialis* is triggered when the cells are exposed to stress conditions such as nutrient starvation, high light intensity, high temperature and salt stress (Aflabo *et al*., 2007; Choi *et al*., 2011; Fábregas *et al*., 1998; Park *et al*., 2014). Astaxanthin accumulation has been induced in *H. pluvialis* during the transformation of the macrozooid cells into non-motile palmella and further into aplanospore (cyst stage), as a response to different stress inducing conditions such as increasing the average cell exposure to light by diluting the culture, increasing the incident light intensity and reducing the light path to the culture, and by nutrient starvation (Figure 4.4).

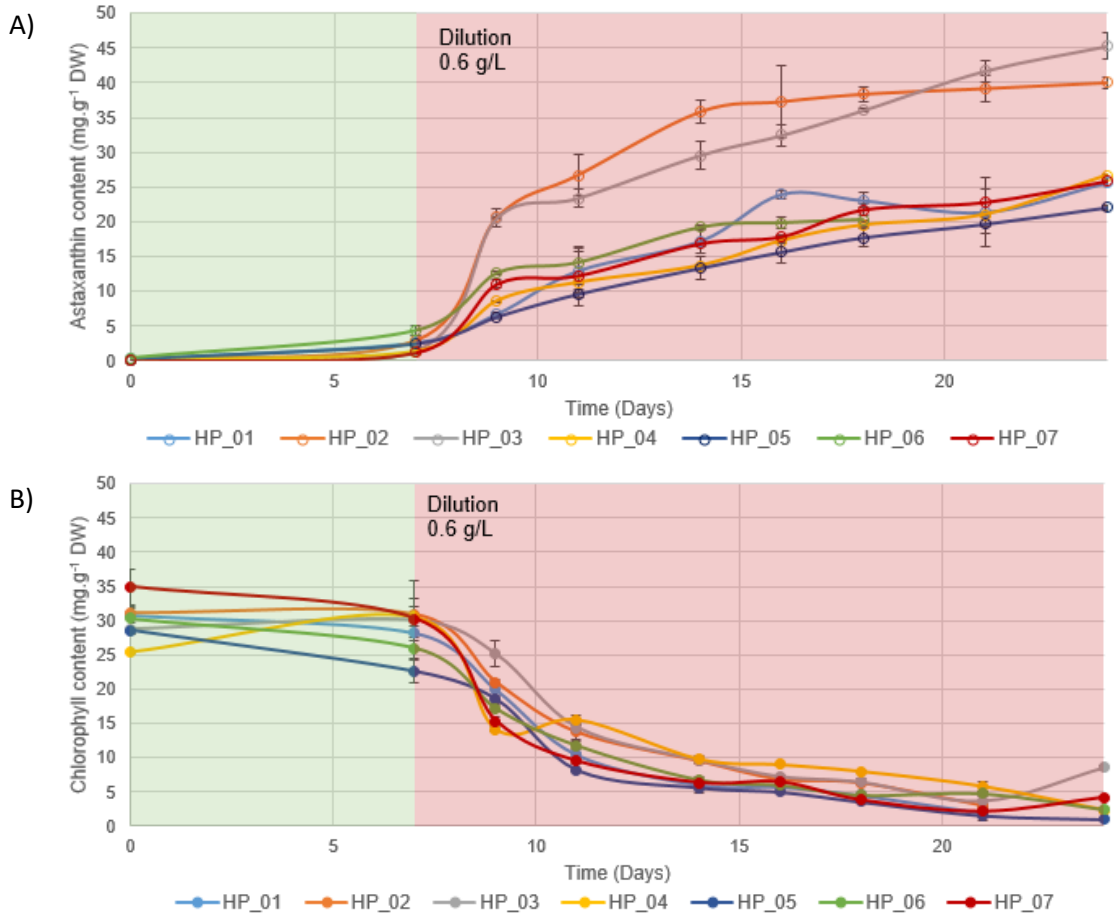

Figure 4.4 – Astaxanthin and chlorophyll contents evolution. Evolution of astaxanthin content (A) and chlorophyll content (B) throughout 24 days of assay. Green background indicates the vegetative stage and optimum conditions; red background indicates the induction stage, with nutrient starvations and high light intensity. Error bars show the based on standard deviation among technical triplicates on pigment analysis.

Figure 4.4A depicts the evolution of astaxanthin content throughout the induction stage for all strains. It can be seen that, between days 9 and 24, a generalized continuous increase of astaxanthin content was observed. It can also be noticed that this global tendency was accompanied by a degradation of

chlorophyll (Figure 4.4B). It is noteworthy that HP_02 and HP_03 strains highlighted by the higher increase in astaxanthin.

Under stress conditions, the highest value of astaxanthin accumulation, 4.4 % (w/w) DW, was reached by the HP_03 strain (Figure 4.5). The strain HP_02 comes next with 3.8 % of astaxanthin, (w/w) DW. The lowest values were observed for strains HP_05 (2.2 % (w/w) DW) and HP_07 (2.6 % (w/w) DW). Astaxanthin content in HP_03 and HP_02 strains presented no statistically significant differences, however, HP_03 was different from the other strains in the study.

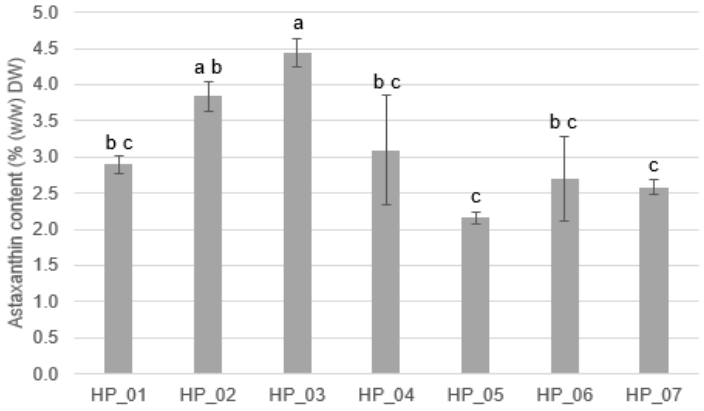

Figure 4.5 – Maximum astaxanthin accumulation. Astaxanthin content achieved after 17 days under stressful condition. Same letters indicate no statistically significant differences and different letters indicate statistically significant differences for $P<0.05$. Error bars show the based on standard deviation among technical triplicate on pigment analyze.

Concerning the astaxanthin productivity after 17 days under stress conditions, HP_03 and HP_02 strains showed the higher astaxanthin productivity, based on the DW, 2.87 ± 0.10 and 2.66 ± 0.31 $mg.g^{-1}$ $DW.day^{-1}$, corresponding to 4.80 ± 0.23 and 4.93 ± 0.19 $mg.L^{-1}.day^{-1}$, respectively (Table 4.3).

The astaxanthin productivity results for all seven strains were lower than those reported in the literature; Zhang *et al*. (2016) obtained a yield of 10.5 mg $astaxanthin.L^{-1}.day^{-1}$, Aflabo *et al*. (2007) reached 11.5 $mg.L^{-1}.day^{-1}$ and the maximum attained in the work of this thesis was 4.93 $mg.L^{-1}.day^{-1}$, for HP_03 strain. However, similar astaxanthin productivities were obtained in a one-step culture process, 3.3 and 5.6 $mg.L^{-1}.day^{-1}$ (Choi *et al*., 2011; Del Río *et al*., 2005). These differences may be the reflex of the light intensity applied during the induction stage, which was much lower than light intensity applied in the other studies, 350 and 500 $\mu mol.m^{-2}.s^{-1}$ (Aflabo *et al*., 2007 and Choi *et al*., 2011), which would surely improve the pigment accumulation and shorten the induction period (García-Malea *et al*., 2005).

Gathering the results obtained: HP_03 and HP_02 were de strains that showed a better performance; and HP_06 and HP_01 were the less productive strains (Table 4.3). Despite this, another way of analyzing the astaxanthin productivity is by comparing the astaxanthin weight per cell. As an interesting fact, HP_06 strain presented the higher cell weight (14438.71 $pg.cell^{-1}$) (Table 4.4), accumulating 389.85 $pg.cell^{-1}$ of astaxanthin, corresponding to 2.7 % of its DW. HP_01 strain was the second strain with higher cell weight, accumulating 301.18 $pg.cell^{-1}$, corresponding to 2.9 % of its DW. HP_06 strain had accumulated more 11 % of astaxanthin per cell than the one described in literature (350 $pg.cell^{-1}$ of astaxanthin) (Zhekisheva *et al*., 2002). According to the literature, aplanospores can reach 3000 $pg.cell^{-1}$ of cell weight, and all strains in this study presented themselves to be heavier that the reported, with the exception of HP_07 (López *et al*., 2006). Comparing the two heaviest strains with the ones with higher astaxanthin productivity, HP_03 strain, had a higher astaxanthin content, 181.37 $pg.cell^{-1}$ of astaxanthin, corresponding to 4.4 % of its DW, and HP_02 strain had accumulated 185.19 $pg.cell^{-1}$ of

astaxanthin, corresponding to 3.8 % of his DW. To sum up, HP_01 and HP_06 might be interesting strains if appropriated conditions are used to enhance their characteristics, in order to benefit from their sizes to improve astaxanthin accumulation and therefore astaxanthin productivity (Fábregas *et al*., 1998)

Table 4.3 – Astaxanthin productivity in mg.g^{-1} DW.day^{-1} and pg.cell^{-1}.day^{-1} after 17 days under stress conditions. Data collected from one assay, representative of the replicates performed. Error based on duplicates of pigments analyzes.

	Astaxanthin Productivity	
	mg.g^{-1} DW.day^{-1}	**mg DW.L^{-1}.day^{-1}**
HP_01	1.35 ± 0.01	2.16 ± 0.01
HP_02	2.31 ± 0.08	4.80 ± 0.23
HP_03	2.58 ± 0.10	4.93 ± 0.19
HP_04	2.00 ± 0.04	2.15 ± 0.10
HP_05	1.16 ± 0.00	1.93 ± 0.04
HP_06	1.52 ± 0.03	3.15 ± 0.02
HP_07	1.26 ± 0.03	1.15 ± 0.02

Table 4.4 – Average of weight per cell. In the beginning and the end of the induction stage.

	HP_01	**HP_02**	**HP_03**	**HP_04**	**HP_05**	**HP_06**	**HP_07**
Initial pg.cell^{-1}	5287.50	1336.16	984.20	1607.34	1096.81	5383.07	845.57
Final pg.cell^{-1}	10385.68	4873.50	4121.99	6411.61	4509.54	14438.71	1285.23

To conclude, despite the higher cell weight obtained for HP_01 and HP_06 strains, the HP_02 and HP_03 strains proved to be the more efficient and profitable to cultivate under the conditions of the two phases tested in order to produce astaxanthin, vegetative growth and induction stages. These two strains were selected and submitted to improvement to achieve the goal of this work.

4.1.3. Additional stress phase

To further enhance the accumulation of astaxanthin, was held a new dilution of the cultures, which were simultaneously subjected to an additional saltine stress (10 ‰ NaCl). The results obtained, after stressing the cells, showed the same behavior as observed before, cessation of growth (Figure 4.2, orange bac*kg*round) and a small increase of astaxanthin accumulation in the majority of the strains after one day in salt medium, with the exception of HP_04 which presented a negative reaction, decreasing their astaxanthin content (Figure 4.6). The enhancement of astaxanthin content occurred in the first day, after cultures have been submitted to a high dilution and salt stress keeping stable for a very short period, of two to three days. Then biomass started to decrease, leading on one hand to a fall in astaxanthin concentration per DW, and on the other, to an increase in pg of astaxanthin per cell. This result can be explained by the amount of energy consumed by the cells, during osmoregulation (Alvensleben *et al*., 2016; Gao *et al*., 2015; Minhas *et al*., 2016; Orosa *et al*., 2001; Sarada *et al*., 2002). Also, possibly to be in the second period of astaxanthin accumulation, the first period corresponds to a rapid astaxanthin accumulation, mainly in free and monoester form; the second period, is characterized by a slower astaxanthin accumulation, mainly in a diester form, corresponding to the larger cell size and higher astaxanthin content per cell (Imamoglu *et al*., 2009; Orosa *et al*., 2001).

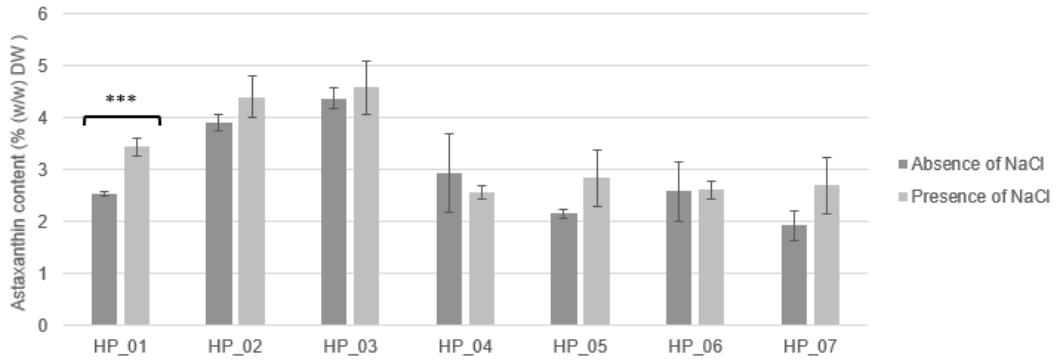

Figure 4.6 – Astaxanthin content through the salinity assay. Dark grey bars present day 0, represents the last value before salt addition. Light grey bars present day 1, represent the first day in the presence of NaCl stress, also represents the day of maximum astaxanthin accumulation. *** indicate statistically significant differences for $P<0.001$. Error bars show the based on standard deviation among technical triplicates of pigment analyzes.

Since additional stress phase did not increase significantly the astaxanthin concentration and led to biomass loss, this additional phase was excluded from the following assays.

4.1.4. Global astaxanthin productivity

Overall astaxanthin productivity was calculated based on the total time required for the astaxanthin accumulation, from the start of the growth phase to the end of the induction stage. It is an important parameter since it gives the real productivity and time for astaxanthin production from *H. pluvialis*, especially in this case where, at the end of growth stage, some cultures have brownish color (Figure 4.1B) due to nutrients depletion. The best results were obtained for HP_03 and HP_02, with 1.88 ± 0.12 $mg.g^{-1}$ $DW.day^{-1}$ and 1.63 ± 0.29 $mg.g^{-1}$ $DW.day^{-1}$, respectively (Table 4.5). Once again, these two strains were the most promising to use in a production regime, due to the fact that, in 24 days of two-stage production (first 7 days for cell growth and 17 days for astaxanthin production and accumulation), they had reach the maximum astaxanthin content. This period of time did not include the astaxanthin accumulation from the salinity stress assay, since it did not present relevant results.

Table 4.5 –Astaxanthin global productivity in $mg.g^{-1}$ $DW.day^{-1}$, presented during 24 days. Data collected from one assay, representative of the replicates performed. Error based on technical duplicates of pigments analyzes.

	Astaxanthin Global Productivity
	$mg.g^{-1}$ $DW.day^{-1}$
HP_01	1.06 ± 0.20
HP_02	1.63 ± 0.29
HP_03	1.88 ± 0.12
HP_04	1.47 ± 0.03
HP_05	0.91 ± 0.08
HP_06	1.01 ± 0.16
HP_07	1,08 ± 0.05

The characterization was completed and HP_02 and HP_03 strains were the ones that showed superior performance in terms of all the analyzed parameters (growth rate, astaxanthin accumulation and productivity). These were the strains selected for cell sorting and UV mutagenesis.

4.2. MONITORING INDUCTION STAGE THROUGH FLOW CYTOMETRY

Flow cytometry analysis is a method that enables relative changes in cell physiological state of microalgae to be detected during a cultivation process. Morphology, including cell size and granularity is influenced by cultivation conditions and correlate with two scattering signals measured by flow cytometry, namely forward scatter (FSC) and side scatter (SSC) signals.

Throughout the induction phase, all the cultures were monitored by flow cytometry. Data first acquisition was made with Flow Max software in a FSC *vs* SSC dot-plot, in which the population was properly identified and gated in order to eliminate artifacts or false events. The Figure 4.7A presents an example of a population gating in a dot-plot graphic using Flow Max prior to further analysis. From this gated population two graphics were obtained: FSC *vs* cell count histogram (Figure 4.7B) and SSC *vs* cell count histogram (Figure 4.7C).

Photosynthetic pigments present in microalgae are chlorophylls and carotenoids, which content depends on cultivation conditions. Pigment fluorescence, the major component of endogenous fluorescence (autofluorescence), has been proven to be linearly related to cellular pigment content (Hyka *et al*., 2013). Therefore, autofluorescence intensity was used for the identification and quantification of microalgae pigments.

For the analysis of pigments autofluorescence, flow cytometric signals were gathered in FL4 and FL2 detectors (FL4 and FL2 *vs* cell count histograms) corresponding to the red fluorescence emitted by chlorophylls and the yellow fluorescence emitted by astaxanthin, respectively, after being excited at 488 nm (Figure 4.7D and E). The histograms show the frequency distributions of fluorescence intensities; where higher fluorescence intensities stand for higher intracellular pigment content. Average values of fluorescence intensities were used for comparison with chemical pigment analysis.

Trigger is a parameter chosen by the user based on a discrimination value (threshold), often FSC, below which events are not considered by the electronic system. The selection of the chlorophyll autofluorescence as a trigger, instead of FSC, allowed excluding cell debris and possible bacterial contaminants, and properly to define the population of interest and set the gates for fluorescence parameters. This trigger does not exclude cells with low chlorophyll content, because these cells always maintain a basal level, detectable by cytometry.

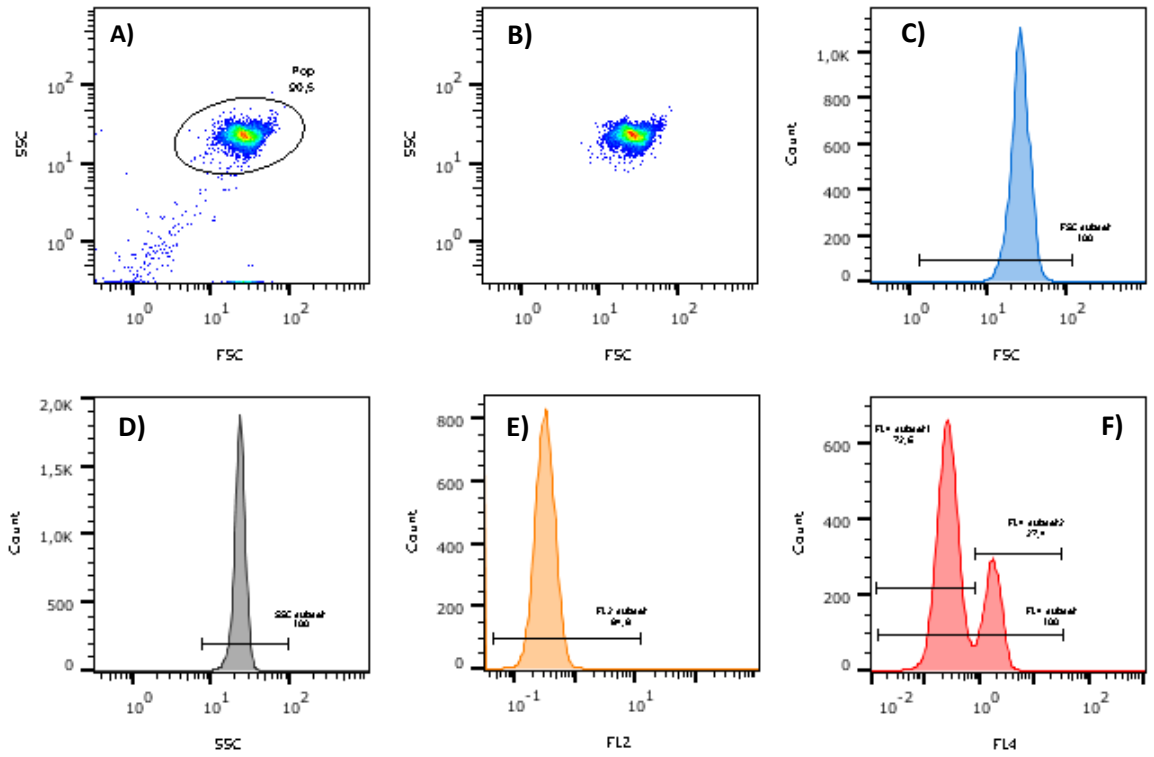

Figure 4.7 – Example of flow cytometric acquisition of HP_03 strain data, on day 0 of induction stage. A) and B) Pseudocolor dot-plot FSC (a.u.) *vs* SSC (a.u.), before and after selecting the population of interest, respectively; C) and D) Scattered signal histograms FSC (a.u.) and SSC (a.u.) *vs* cell count, respectively; E) Astaxanthin autofluorescence (FL2 detector – 575 nm) histogram; E) Chlorophyll autofluorescence (FL4 detector – 675 nm) histogram. a.u.: arbitrary units.

Figure 4.8 presents a multiparametric analysis comparing the results obtained in the characterization of the 7 strains of microalgae at the beginning (day 0) of the induction phase. The results have revealed the existence of two sub-populations in the culture of HP_06 strain, characterized by different dimensions (FSC), complexities (SSC), chlorophyll (FL4) contents and astaxanthin (FL2) presence. The subpopulation of smaller, less complex and with less chlorophyll content may correspond to injured cells and cells lacking part of its contents.

Interestingly, it was found that in general, with the exception of the afore mentioned HP_06 strain, at the beginning of the induction stage, the strains showed little variability in terms of sizes, complexities, astaxanthin content and chlorophyll presence (Figure 4.8). It should also be noted that, with the exception of HP_01 strain, which was presented as a single population with a high chlorophyll content, in all other strains were identified two subpopulations of cells with different levels of chlorophyll (Figure 4.8D); for HP_02, HP_04 and HP_07 strains, the two subpopulations were equivalent (about 50 %), whereas for the other strains was observed a predominant subpopulation with lower chlorophyll content.

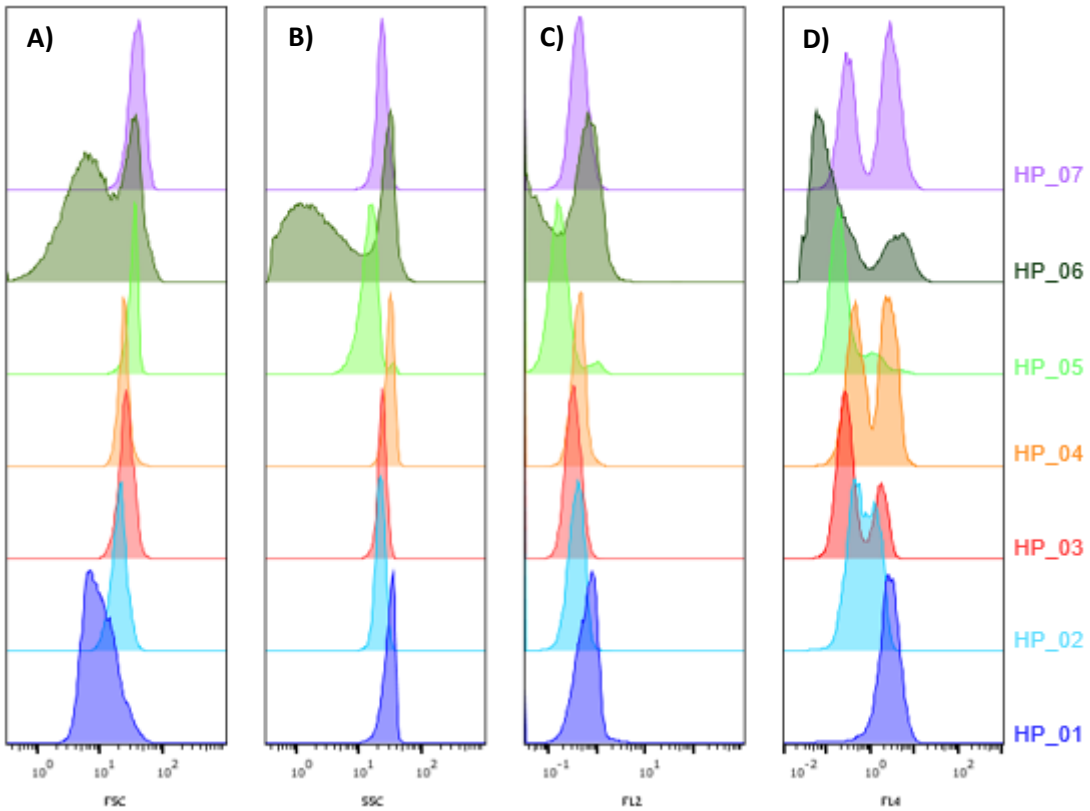

Figure 4.8 – Flow cytometry comparison of the seven strains on day 0 of induction stage. A) and B) scattered signals FSC (a.u.) and SSC (a.u.) *vs* cell count histogram; C) and D) autofluorescence of astaxanthin (FL2 (a.u.)) and chlorophyll (FL4 (a.u.)) *vs* cell count histogram. a.u.: arbitrary units.

Microalgae cultures of the 7 strains were monitored by flow cytometry throughout the induction phase, to follow the evolution of the physiological state of the cells and monitoring the accumulation of astaxanthin (Figures 4.9 to 4.12).

Figure 4.9 depicts the evolution of HP_01 culture over the induction stage. As can be seen, in this culture was not detected any change in the complexity or granularity of the cells (Figure 4.9B), and it was observed a temporary increase in cell size by the 4th day of induction (Figure 4.9A) and at the end of the stage. Regarding the pigments content, it was visible a uniform increase of astaxanthin from the 2nd day and a decrease in chlorophyll content from the 7th day of induction (Figure 4.9C and D respectively). HP_02 and HP_04 strains presented identical behavior (data not shown).

Despite the marked similarity in the evolution of the physiological features of the HP_03 strain (Figure 4.10), in particular relatively to the granularity of the cells (Figure 4.10B) and astaxanthin content (Figure 4.10D), this strain exhibited some differences in the following aspects: the target population showed greater heterogeneity regarding the cells size, between day 7 and day 14 of the induction period, corresponding to an increase of astaxanthin and a progressive reduction in the chlorophyll content (Figure 4.10A, C and D). It is noted that, on the 4th day of this phase, were observed three distinct subpopulations of cells with different levels of chlorophyll.

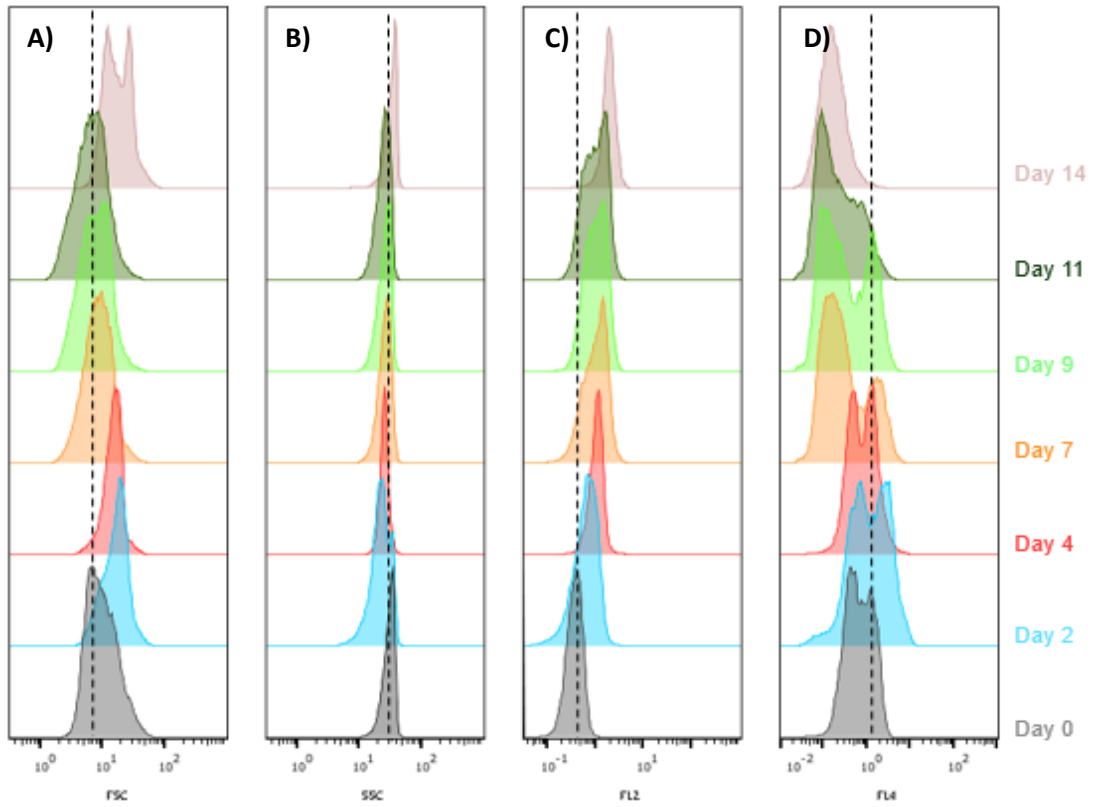

Figure 4.9 – Multiparametric analysis of the evolution of HP_01 cells physiological state, throughout the induction stage. The dot line marks the day 0 of induction stage. A) and B) scattered signals FSC (a.u.) and SSC (a.u.) vs cell count histogram, respectively; C) and D) autofluorescence of astaxanthin (FL2 (a.u.)) and chlorophyll (FL4 (a.u.)) vs cell count histogram, respectively. a.u.: arbitrary units.

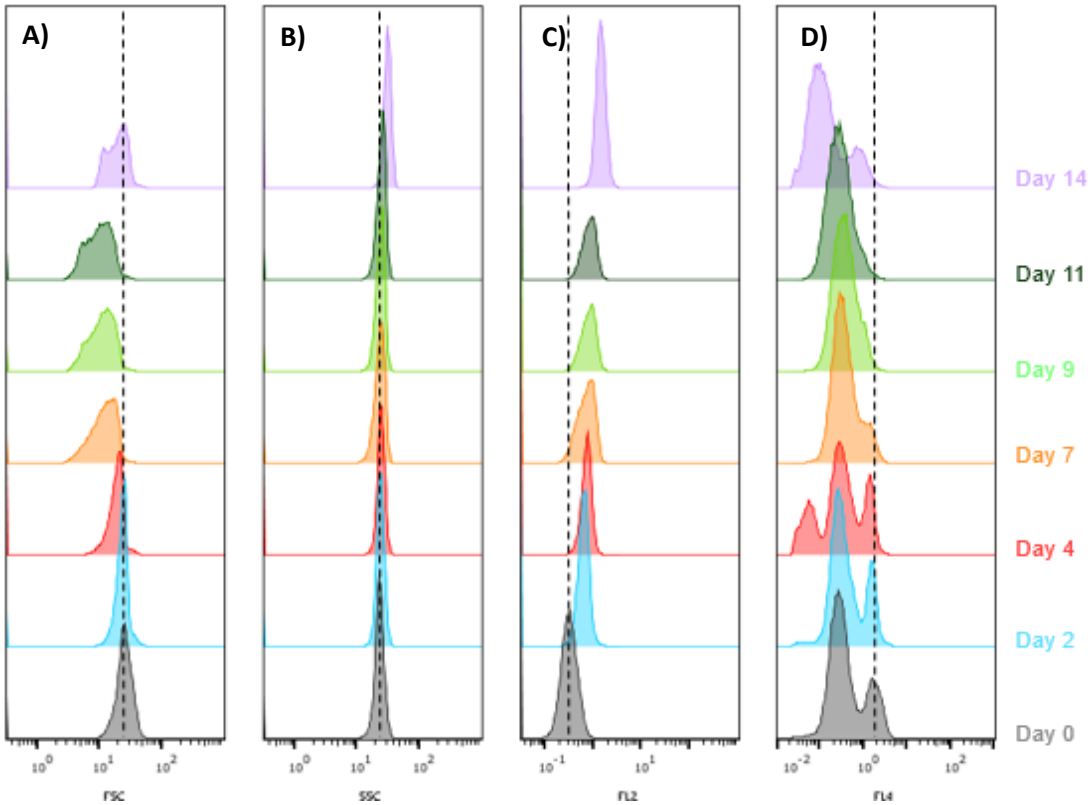

Figure 4.10 – Multiparametric analysis of the evolution of HP_03 cells physiological state, throughout the induction stage. The dot line marks the day 0 of induction stage. A) and B) scattered signals FSC (a.u.) and SSC (a.u.) *vs* cell count histogram, respectively; C) and D) autofluorescence of astaxanthin (FL2 (a.u.)) and chlorophyll (FL4 (a.u.)) *vs* cell count histogram, respectively. a.u.: arbitrary units.

The evolution of HP_05 strain culture was characterized by a great uniformity in the size and cell complexity (Figure 4.11A and B), in contrast to the marked increase in astaxanthin content observed from day 2 of induction, together with the foreseeable decreased content of chlorophyll (Figure 4.11C and D).

HP_07 was the only strain that showed a distinct behavior (Figure 4.12), characterized by a gradual decrease in cell size and complexity (Figure 4.12A and B), as well as a sharp decrease in chlorophyll content from the 2nd day of induction stage (Figure 4.12D). Interestingly, the observed increase of the astaxanthin content was barely noticeable (Figure 4.12C), which is consistent with previous results obtained for astaxanthin accumulation rate and for the pigment content quantified by the method of total pigments extracted.

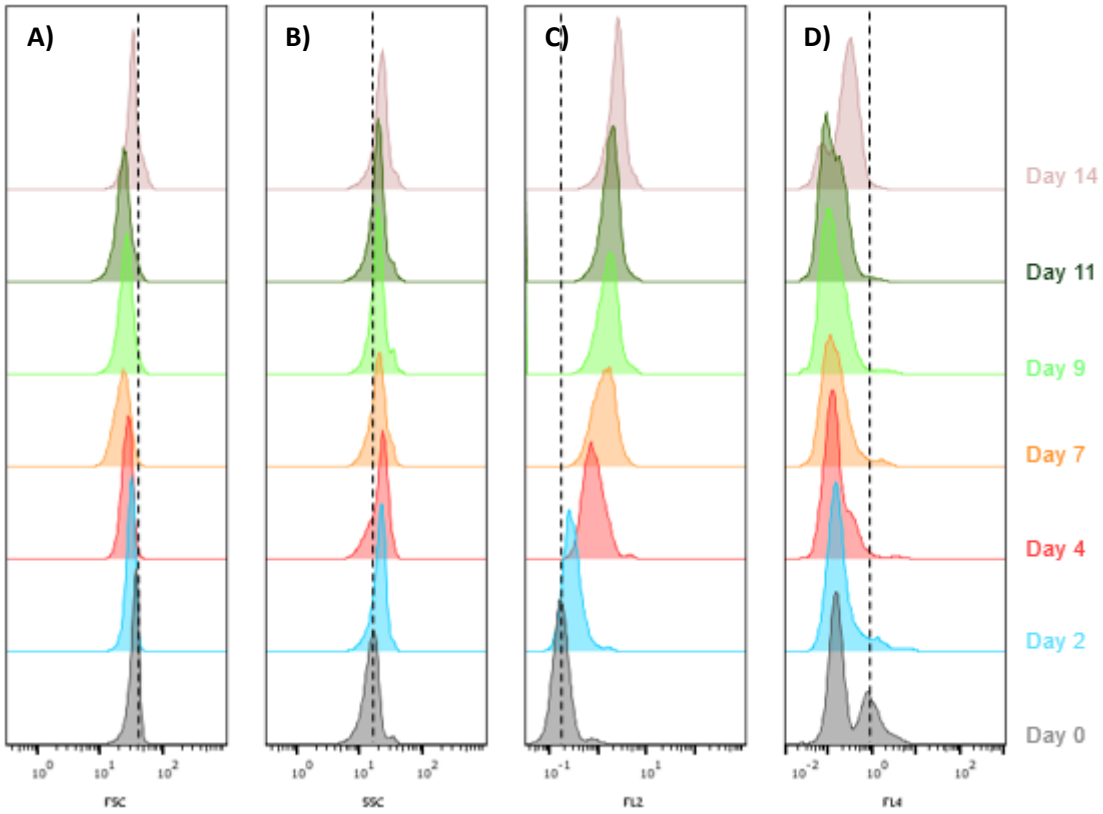

Figure 4.11 – Multiparametric analysis of the evolution of HP_05 cells physiological state, throughout the induction stage. The dot line marks the day 0 of induction stage. A) and B) scattered signals FSC (a.u.) and SSC (a.u.) vs cell count histogram, respectively; C) and D) autofluorescence of astaxanthin (FL2 (a.u.)) and chlorophyll (FL4 (a.u.)) vs cell count histogram, respectively. a.u.: arbitrary units.

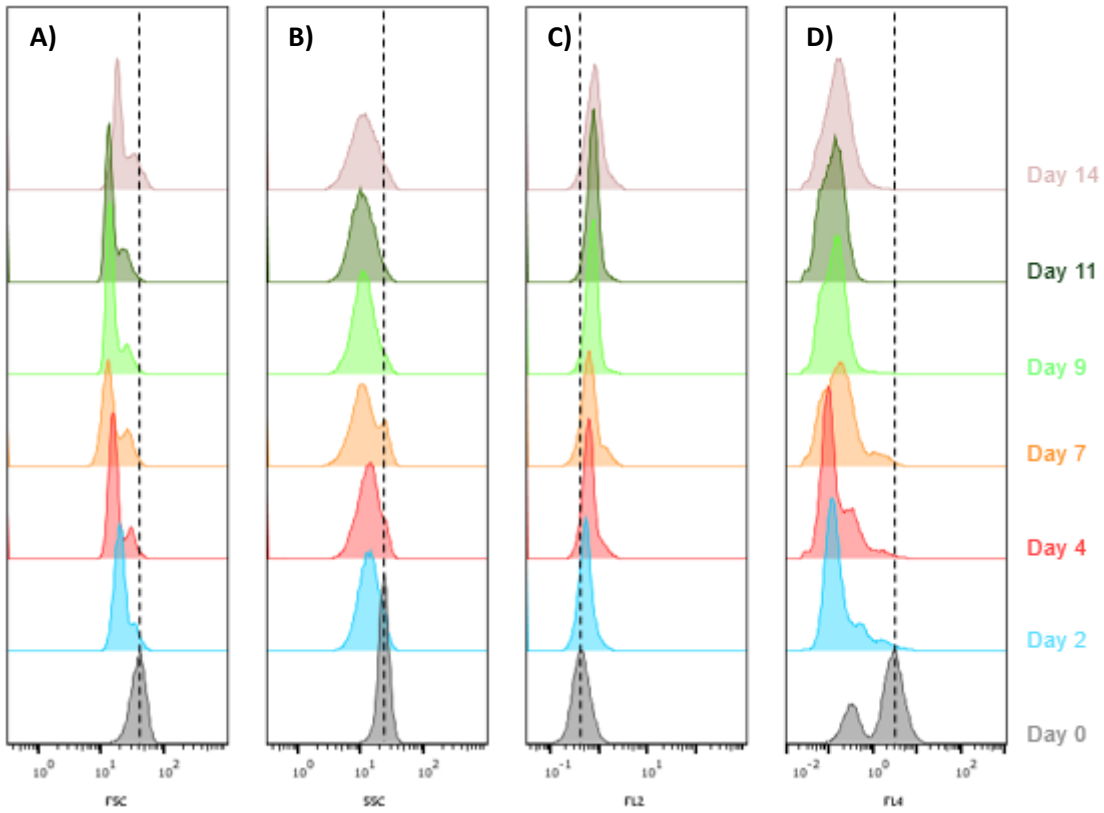

Figure 4.12 – Multiparametric analysis of the evolution of HP_07 cells physiological state, throughout the induction stage. The dot line marks the day 0 of induction stage. A) and B) scattered signals FSC (a.u.) and SSC (a.u.) *vs* cell count histogram, respectively; C) and D) autofluorescence of astaxanthin (FL2 (a.u.)) and chlorophyll (FL4 (a.u.)) *vs* cell count histogram, respectively. a.u.: arbitrary units.

The results of astaxanthin quantification by flow cytometry (average values of fluorescence intensities) were consistent with those determined by total pigments extraction method. A linear correlation was found (r = 0.96) between the full set of astaxanthin content values obtained with the two methods (Figure 4.13).

The reported results showed that, flow cytometry technique allowed *H. pluvialis* cultures evolution to be monitored during the encystment process, based on morphological and physiological parameters; further demonstrated that autofluorescence of astaxanthin is a good indicator of intracellular accumulation of this pigment, and therefore can be monitored in real time by flow cytometry.

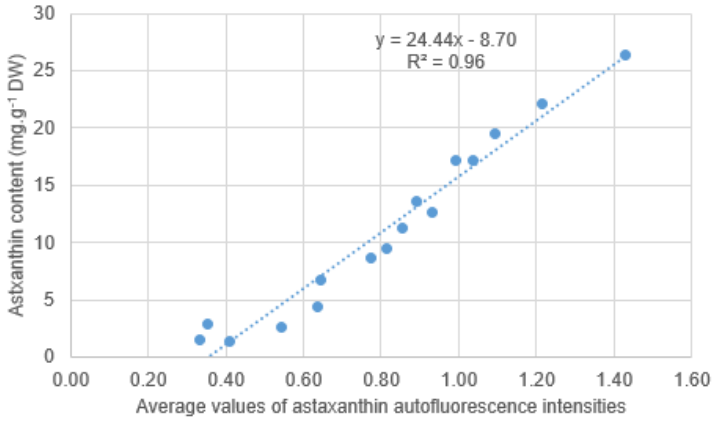

Figure 4.13 – Correlation between astaxanthin content quantified by total pigments extraction, and autofluorescence intensity (arbitrary units) determined by flow cytometry. The relation between the two methods was characterized by a linear function (dotted line).

4.3. SELECTION AND SORTING CELLS OF INCREASED ASTAXANTHIN CONTENT

Monitoring physiological changes of microalgae during cultivation process by flow cytometry allowed the determination of optimal conditions to reach the target maximum astaxanthin content. Potentially, overproducer subpopulations isolated from a heterogeneous culture can be cultivated again and further analyzed. As a major tool for cell sorting, flow cytometry, especially fluorescence-activated cell sorters (FACS), has been widely exploited for the physical separation of cells of interest that differ in cell size, morphology, or fluorescence (Basu *et al*., 2010; Pappas and Wang, 2007).

The screening of the 7 strains of *H. pluvialis*, carried out by monitoring and characterization of cultures throughout vegetative growth and induction stages, allowed selecting HP_02 and HP_03 as the most promising strains in terms of performance and increased astaxanthin production. Analyzing the results, HP_02 and HP_03, presented the higher values of growth rate, biomass productivity, astaxanthin content and productivity, being selected to perform cell sorting for enrichment of overproducer cells.

The Partec sorter has a flow chamber with a piezo element and an electronic device for piezoelectric activation. The diamond piezo deflects the sorted cells into a second branch of the flow cell. In the sample flow each cell is analyzed and all the signals reach the computer, where the decision is made which cell should be sorted, according to the software gating. Time of acquisition was set to enhance the yield and purity of the subpopulation to be collected. The acquisition was executed at less than 300 events per second, allowing a high precision on selection.

At the end of the induction stage, when the cells reached the maximum astaxanthin autofluorescence, a sample was taken, to be analyzed and sorted. The first step was to identify the parameter settings that allowed the best visualization of the interest population and to check the sorting efficiency. A broad two-dimensional gating logic has been defined by astaxanthin content (FL2) and size (FSC), in a pseudo-color dot plot (Figure 4.14). At the end of the sort, a portion of the sorted cells has been re-analyzed to assess the purity and recovery of the sort and how efficient the sort was in terms of cell yield. The purity of the sort was evaluated by analyzing the cells in the sorted tube and by assessing the percentage of cells that fulfill the sort criteria. The sort recovery was defined, as the percentage of events that the sort counters had indicated which actually ended up in the sorted tube.

In Figure 4.14, the gate represents the thresholds used by sorting unit to physically separate the target cells. For HP_02 and HP_03 have been selected to collect, only 1.03 % and 1.33 % of the total events respectively. It is noteworthy that, cell sorting had limited discrimination power to the cultures submitted due to the population homogeneity. The outlier cells with increased astaxanthin contents, corresponding to less than 1.5 % of the whole population. The selected events only represented 19 % of the total cells sorted (Figure 4.15).

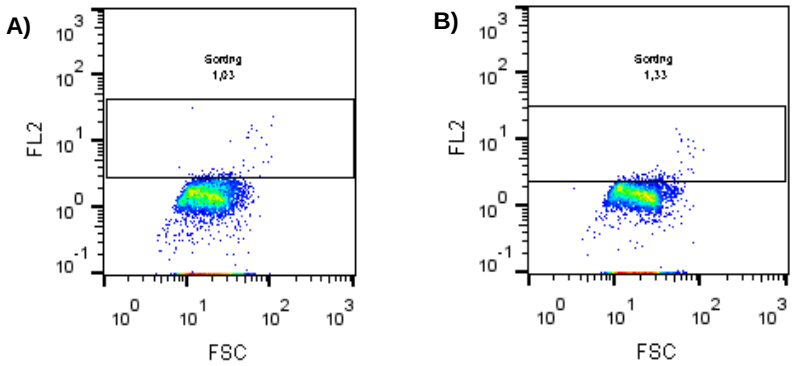

Figure 4.14 – Defined gate to perform cell sorting. FSC (a.u.) against FL2 (a.u.) was used to define the events to be sorted. A) sample of HP_02 and B) sample of HP_03. a.u.: arbitrary units.

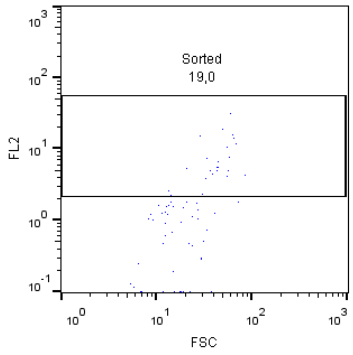

Figure 4.15 – Sample from HP_03 sorted cells. The same gate *Sorted* represents the cells of interest (19%).

When two districted subpopulations are intending to separate, cell sorting is usually performed with success (Pereira *et al*., 2011; Terashima *et al*., 2015). However, in this work, as it can be seen in Figure 4.13, the cells selected by the gate depicted showed high values of astaxanthin autofluorescence, possibly because they were also the biggest cells within the population, which can be evidenced by its light scattering (FSC values) in comparison with the whole population. In the relatively homogeneous populations, much of the variation in the astaxanthin content of individual cells was due to extrinsic noise factors such as cell size. Cell sorting is a technique that presents a high output, however, it still needs further work when performed in the isolation of cells in monocultures to increase its efficiency (Sinigalliano *et al*., 2009).

Partec flow cytometer is equipped with two excitation sources, one of 488 nm (blue laser) and the other of 635 nm (red laser), which excites chlorophyll fluorescence (far red autofluorescence) in microalgae. The two lasers are in a non-co-linearity system (one plan by excitation source), which allows effective fluorescence splitting, but create a spatial gap, electronically converted to a temporal gap (time laser delay) to synchronize different light signals from one cell.

As already mentioned, the selection of the chlorophyll autofluorescence as a trigger, instead of FSC, allowed excluding cell debris and possible bacterial contaminants, and properly to define the population of interest and set the gates for fluorescence parameters. However, this selection, associated to the population homogeneities, made it impossible to carry out an efficient sorting due to the non-synchronization of the chlorophyll autofluorescence signal in the far red detected in FL4.

4.4. RE-CULTIVATION THE CULTURES SUBMITTED TO CELL SORT

The cell sorting was carried out using sterile sheath fluid and sterile vials to collect sorted cells so as to allow subsequent culture. After sorting, the isolated cells have been transferred to an appropriate sterile medium in order to allow their recovery and then were placed in a scale-up regime to reach the necessary volume to begin a new assay. This new assay was done to compare the sorted cells with the original population, using the same experimental set-up.

The collected cells showed no differences when compared to the original population (Table 4.6) and did not show improvement in the analyzed parameters (growth rate, biomass productivity, maximum astaxanthin content and productivity). However, sorted cells grew as well as control cells, despite the mechanical stress of the sorting and the reduced number of cells.

Table 4.6 – Original culture *vs* culture from cell sort. Principal parameters analyzed were growth rate (day^{-1}), biomass productivity ($mg.L^{-1}.day^{-1}$), maximum astaxanthin content (% (w/w) DW) obtained during the whole assay and astaxanthin productivity ($mg.g^{-1}$ $DW.day^{-1}$) along 17 days of induction phase.

HP_03	Growth rate (day^{-1})	Biomass Productivity ($g.L^{-1}.day^{-1}$)	Maximum Astaxanthin content (% (w/w) DW)	Astaxanthin Productivity ($mg.g^{-1}$ $DW.day^{-1}$)
Original Cultures	0.58 ± 0.22	0.22 ± 0.02	4.4 ± 0.34	2.87 ± 0.10
Cultures sorted	0.45 ± 0.17	0.17 ± 0.02	4.4 ± 0.10	2.57 ± 0.07

4.5. MUTAGENESIS

Induced cell mutagenesis and mutant selection have been suggested as a method for microalgae strain improvement (Chen *et al*. (2003) and Kamath *et al*. (2008)). Algal mutants could be obtained by UV radiation for enhancing astaxanthin production. UV-C light (254 nm) promotes DNA damage and random mutations and has an advantage of not being classified as a genetically modified method.

4.5.1. Response of *H. pluvialis* to UV mutagenesis

A preliminary random mutagenesis assay was performed using HP_03 *H. pluvialis* strain since it was the most promising of the seven strains.

The lethality effect of UV exposure time was studied by subjecting HP_03 vegetative green cells to UV-C radiation for different time periods (see section 3.5). Cell viability was evaluated by flow cytometry with an oxonol fluorescent stain, which allowed analyzing the effect of the functional integrity of the membrane. Bis-(1,3-Dibutylbarbituric Acid) Trimethine Oxonol ($DiBAC_4(3)$) is a slow-response potential-sensitive probe that can enter depolarized cells, where it binds to intracellular proteins or membrane and exhibits enhanced green fluorescence (FL1). Increased membrane depolarization determining an additional entry of the stain with the concomitant increase in fluorescence. Conversely, metabolically active viable cells, having a membrane potential (negative inside) exclude the oxonol probe, which is indicated by a decrease in fluorescence (Krujatz *el al*., 2015).

The results obtained from the flow cytometric analysis, summarized in the Figure 4.16, allowed following the evolution of cellular viability with the increasing exposure to UV radiation. As it can be seen in Figure 4.16A, in the control sample, not subject to UV exposure, most cells of the population of interest (≈ 90 %) were metabolically active and energized. However, it was possible to differentiate two subpopulations with different vitality: a subpopulation with a higher membrane potential (lower fluorescence intensity – 55 %), and a less energized subpopulation (greater fluorescence intensity – 38 %).

The exposure to UV radiation determined a progressive depolarization of the membrane, which was translated by a shift of the green fluorescence to values of greater intensity, clearly visible in Figure 4.16B and C. In the 40 s of exposure (Figure 4.16B), it was possible to differenciate two subpopulations, one of which, with lower green fluorescente (lower fluorescence intensity detected in FL1) corresponding to metabolotically active and energized cells (≈ 60 % of the global population). It should be noted that at the end of 100 s of UV exposure, a generalized dissipation of the membrane potential was observed.

Viability was also determined by Muse® cell analyzer, using propidium iodide (PI) as a staining dye for dead cells. PI is membrane impermeant and generally excluded from viable cells and binds to nucleic acids by intercalating between the bases with little or no sequence specificity; once the dye is bound to nucleic acids, its red fluorescence (FL3) is enhanced.

The results of flow cytometry viability analysis (% of energized membranes) were consistent with those obtained by Muse® cell analyzer (% cells with undamaged membranes). A linear correlation was found (r = 0.99 between the full set of viability values obtained with the two methods (Figure 4.17), and the last one have been selected to perform the dose-response curve of *H. pluvialis*.

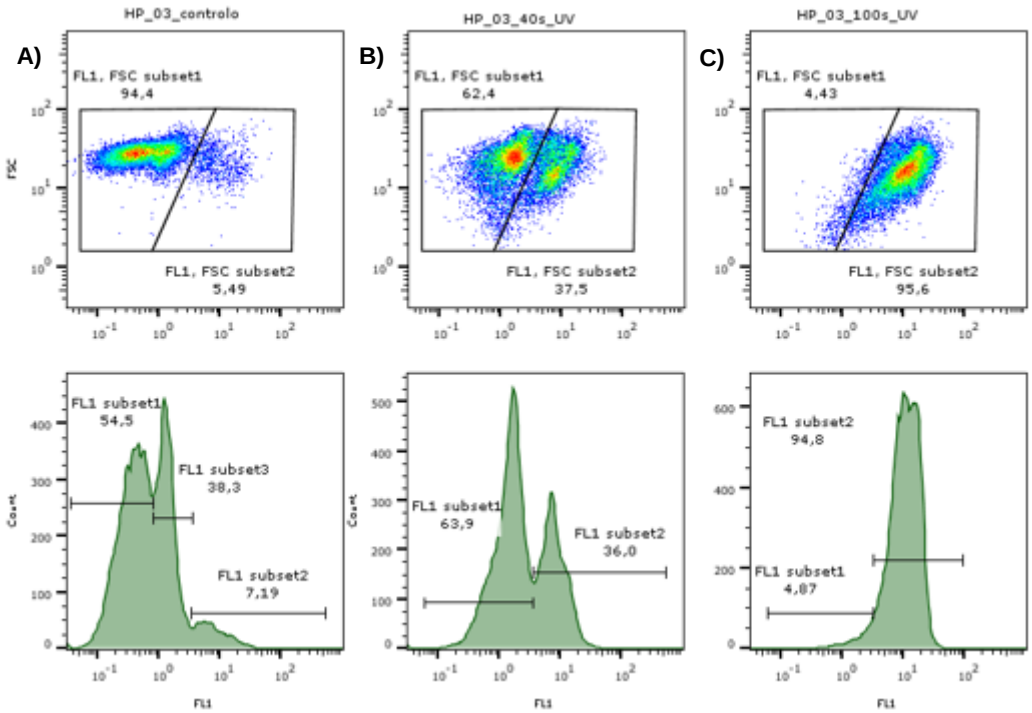

Figure 4.16 – Evaluation of *H. pluvialis* viability during the exposition to 40 and 100 s of UV radiation. Pseudocolor plots of HP_03 DiBAC$_4$(3) stained cells, FSC (a.u.) *vs.* FL1 (a.u.) and the mono-parametric histograms of green fluorescence: A) control; B) 40 and C) 100 s of UV radiation exposure; a.u.: arbitrary units.

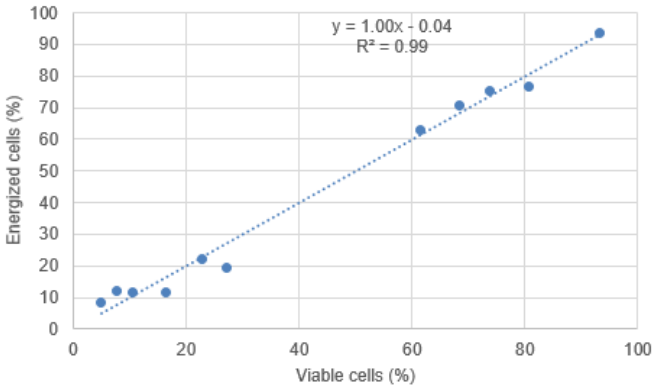

Figure 4.17 – Correlation between the viability determined by Muse® cell analyzer with PI and from Flow Cytometry with DiBAC$_4$(3). The relation between the two methods was characterized by a linear function (dotted line, r = 0.99).

4.5.2. Dose-response curve determination

As already mentioned above, the lethality effect of UV exposure time was studied by subjecting HP_03 vegetative green cells to UV-C radiation for different time periods. The survival rate was dependent on the UV exposure time, and the prolonged exposure led to lower survival rate (Figure 4.18). It was found that 40 s of UV exposure time resulted in approximately 60 % survival rate while 90 % survival rates were achieved upon 70 s UV treatment. Exposure time of 70 s was chosen for further UV mutagenesis assays.

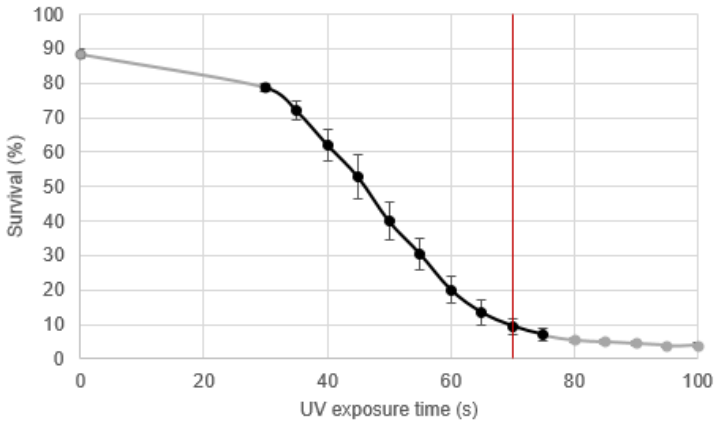

Figure 4.18 – Dose-response curve of *H. pluvialis* to UV light exposure. The black vertical line mark the lethal dose to reach 10 % of viability. Error bars show the uncertainty based on standard deviation between triplicate counts on cytometry Muse® cell analyzer.

4.5.3. Two-stage cultures for the production of astaxanthin

Three cultures of HP_03 strain were submitted to 70 s of UV-C radiation and were immediately kept at dark conditions over night to prevent photo reactivation, and then placed in scale-up regime to achieve enough volume to transfer to bubble columns. The experimental strategy used was the two-stage cultivation, where the third terminal phase of additional saline stress was not performed in this situation. In the first phase, during seven days, the cultures presented the same evolution as the control (Figure 4.19, green bac*kg*round). Maximum cell density obtained was 1.77×10^6 cell.ml^{-1} from HP_03, although, it started with a higher cellular concentration than the other cultures. Mut 1, Mut 2 and Mut 3, reach the maximum cellular densities of 1.29×10^6, 1.08×10^6 and 1.57×10^6 cell.ml^{-1}, respectively.

In the beginning of induction stage, the cultures were diluted to 0.6 $g.L^{-1}$. The mutant's evolution was similar to the control, under stress the cellular density remained unchanged (Figure 4.19, red bac*kg*round). The results obtained, shown that after the UV exposure, cultures were superior to the control in all parameters, growth rate, astaxanthin productivity and accumulation, and biomass productivity kept the same. Mutants were also monitored, during the induction stage, by flow cytometry, however, the differences in the heterogeneity of UV exposure population had not increased.

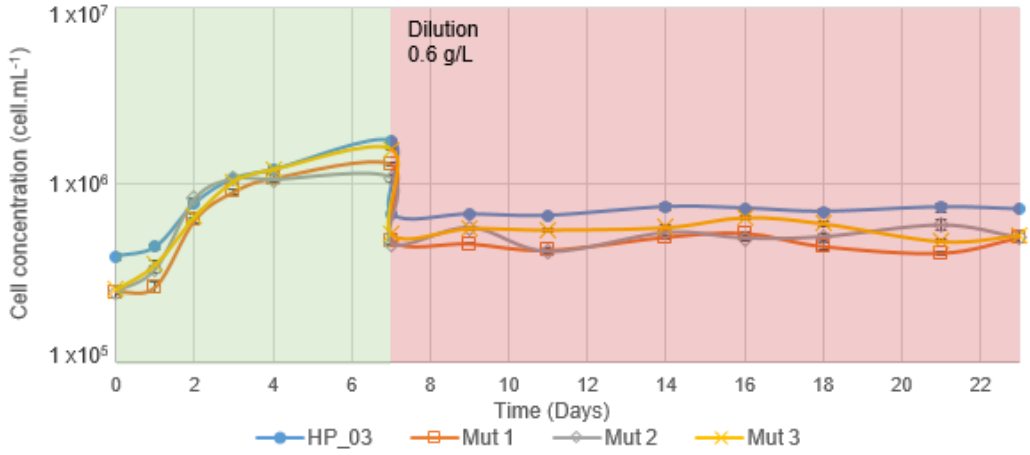

Figure 4.19 – Cultures evolution during the assay. Evolution of cellular concentration throughout the 30 days of assay; culture conditions corresponding to the three stages: green bac*kg*round indicates the vegetative stage and optimal conditions; red bac*kg*round indicates the induction stage, with nutrient starvation and high light intensity. Error bars show the uncertainty based on standard deviation among triplicates on Neubauer Chamber counting.

4.5.3.1. Characterization of Vegetative Growth Stage

Mut 1 and Mut 3 presented the higher values of growth rate, 0.45 and 0.41 day^{-1}, respectively. In terms of biomass productivity, all the cultures obtained the same values (Table 4.7). According to the literature and as it was discussed before, the values obtained in this assay were lower in terms of growth rate and the identical for the biomass productivity (Aflabo *et al*., 2007; Garcia-Malea *et al*., 2006; Kaewpintong *et al*., 2007; Kobayashi *et al*., 1992).

Table 4.7 – Growth rate and biomass productivity in the vegetative growth stage. Based on one tests to each sample submitted to the same cultivation conditions.

	HP_03	**Mut 1**	**Mut 2**	**Mut 3**
Growth rate (day^{-1})	0.34 ± 0.02	0.45 ± 0.03	0.39 ± 0.02	0.41 ± 0.02
Biomass productivity ($g.L^{-1}.day^{-1}$)	0.19 ± 0.03	0.21 ± 0.03	0.17 ± 0.03	0.22 ± 0.03

At the beginning of the assay, the total chlorophyll, content was greater than 52 mg.g-1 DW and carotenoids were less than 15 mg.g-1 DW. The maximum chlorophyll content was observed in Mut 1, 61.24 ± 1.40 mg.g-1 (6.1 % (w/w) DW), which also showed the maximum total carotenoid content, 14.64 ± 0.28 mg.g-1 (1.5 % (w/w) DW) (Table 4.8). These values were higher than the previously reported by other authors, who reported for green cells an average chlorophyll content of 2.4 ± 0.11 % (w/w) DW and an average primary carotenoid content of 0.48 ± 0.03 % (w/w) DW (Grewe and Grield, 2008).

Table 4.8 – Total of chlorophylls and carotenoids in the vegetative growth stage in the first day. Total chlorophylls comprise chlorophyll a and b; Total carotenoids comprise astaxanthin, cantaxanthin, neoxanthin, violaxanthin, lutein, zeaxanthin and β-carotene. Errors were based on standard deviation of triplicates from pigment analysis.

Vegetative stage	Total Chlorophylls (mg/g)	Total Carotenoids (mg/g)
HP_03	52.79 ± 4.02	13.40 ± 0.84
Mut 1	61.24 ± 1.40	14.64 ± 0.28
Mut 2	60.37 ± 9.81	13.69 ± 1.31
Mut 3	54.48 ± 7.52	13.93 ± 1.25

4.5.3.2. Characterization of Induction Stage

In the last day of induction stage, maximum astaxanthin accumulation observed was 4.1 % (w/w) DW, in Mut 2. When comparing results from mutants to the control, the mutants accumulate more astaxanthin: Mut 1 (3.7 % (w/w) DW), Mut 2 (4.1 % (w/w) DW), Mut 3 (3.9 % (w/w) DW) and the control (3.1 % (w/w) DW). Also, the mutants presented higher astaxanthin productivy: Mut 1 (2.12 ± 0.09 $mg.g^{-1}$ $DW.day^{-1}$), Mut 2 (2.46 ± 0.07 $mg.g^{-1}$ $DW.day^{-1}$) and Mut 3 (2.26 ± 0.09 $mg.g^{-1}$ $DW.day^{-1}$), the control presented a productivity of 1.85 ± 0.09 $mg.g^{-1}$ $DW.day^{-1}$ (Table 4.9). Mut 2 presented the higher values in the induction phase, its astaxanthin global productivity was 1.71 ± 0.01 $mg.g^{-1}$ $DW.day^{-1}$, during 24 days of *H. pluvialis* production. However, as discussed in the previous assays, the productivities obtained were lower than the ones reported in the literature (Aflabo *et al*., 2007).

Table 4.9 – Maximum astaxanthin content, astaxanthin productivity and global productivity. Astaxanthin productivity was measured during the 17 days of induction and the astaxanthin global productivity was measured during the 24 days of assay. Error based on uncertainty of standard deviation between triplicates on pigments analysis.

Induction Stage	Astaxanthin Content		Astaxanthin Productivity		Global Productivity
	$mg.g^{-1}$ DW	% (w/w) DW	$mg.g^{-1}$ DW $.day^{-1}$	$mg.L^{-1}.day^{-1}$	$mg.g^{-1}$ DW $.day^{-1}$
HP_03	30,78 ± 1,12	3.1	1.85 ± 0.09	5.56 ± 0.02	1.28 ± 0.01
Mut 1	37.22 ± 0.66	3.7	2.12 ± 0.09	3.68 ± 0.03	1.55 ± 0.02
Mut 2	41.04 ± 1.04	4.1	2.46 ± 0.07	3.06 ± 0.13	1.71 ± 0.01
Mut 3	38.67 ± 0,72	3.9	2.26 ± 0.09	2.56 ± 0.20	1.61 ± 0.02

4.5.3.2.1. Monitoring induction stage through flow cytometry

The new populations generated presented a similar behavior when compared to the control (Figure 4.20 and 4.21). This cultures had a decreased in pH (around of 6.15) during a couple of days and the cells might have undergone morphological changes presenting differences from the previous assay realized. In the present assay, as observed in FSC channel presented an increase of variation and diminution of cell size. The complexity of the population remains constant as the previous assay and the FL2 increase over the induction stage. FL4 channel did not present variation during the assay (Figure 4.21).

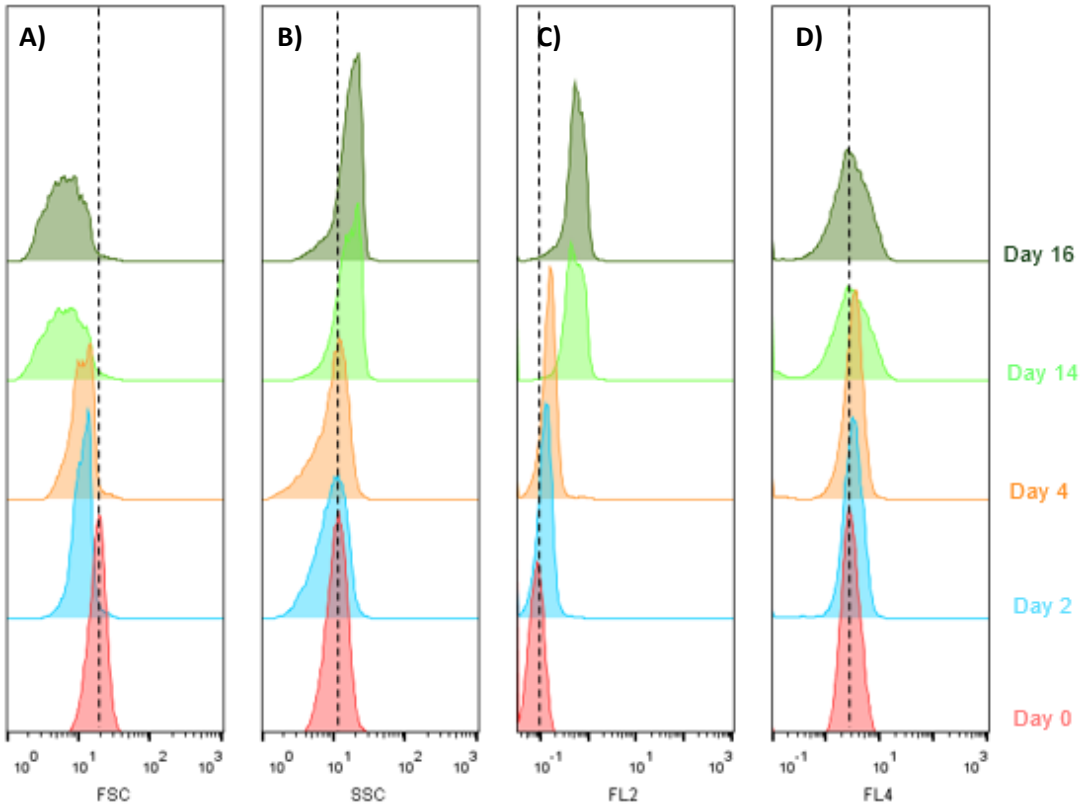

Figure 4.20 – Multiparametric analysis of the evolution of HP_03 cells physiological state, throughout the induction stage. The dot line marks the day 0 of induction stage. A) and B) scattered signals FSC (a.u.) and SSC (a.u.) *vs* cell count histogram, respectively; C) and D) autofluorescence of astaxanthin (FL2 (a.u.)) and chlorophyll (FL4 (a.u.)) *vs* cell count histogram, respectively. a.u.: arbitrary units.

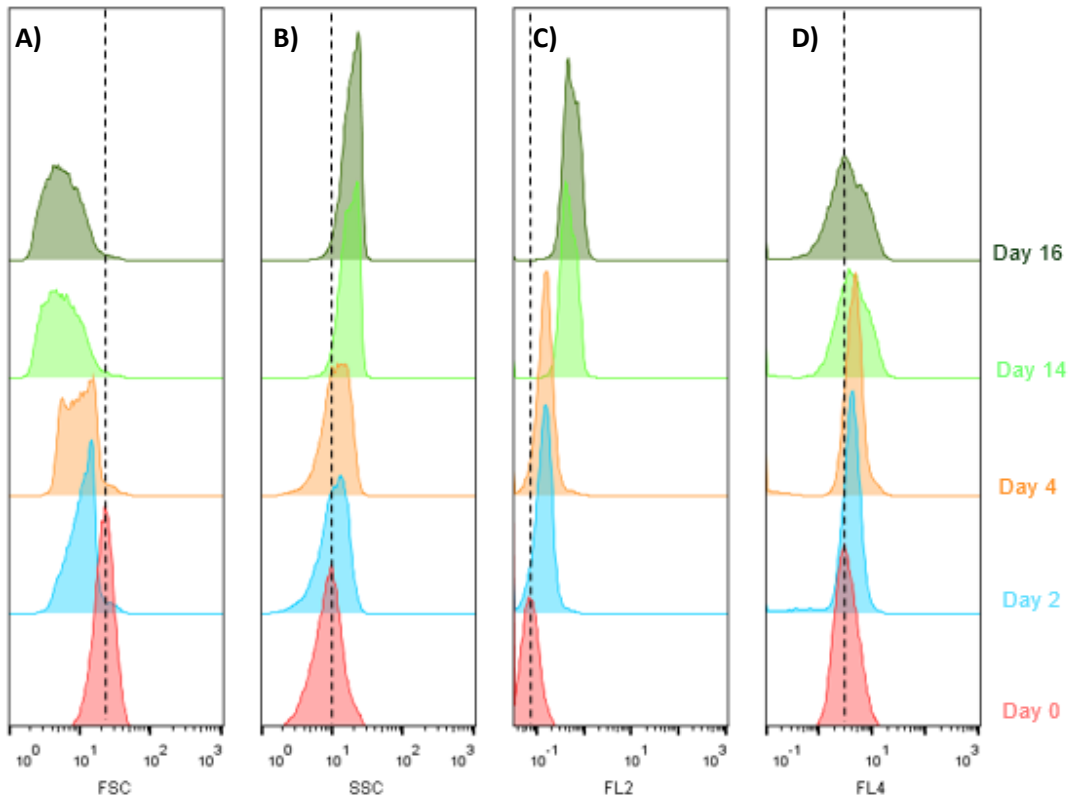

Figure 4.21 – Multiparametric analysis of the evolution of Mut 2 cells physiological state, throughout the induction stage. The dot line marks the day 0 of induction stage. A) and B) scattered signals FSC (a.u.) and SSC (a.u.) *vs* cell count histogram, respectively; C) and D) autofluorescence of astaxanthin (FL2 (a.u.)) and chlorophyll (FL4 (a.u.)) *vs* cell count histogram, respectively. a.u.: arbitrary units.

According to the literature, for a successful mutagenesis strategy there needs to be a combination of an efficient method of generating random mutations and an efficient strategy that permits screening of the desired phenotypes. For this assay, the cultures were only exposed one time to UV irradiation and thus further rounds of mutagenesis may be needed. For screening, as UV exposed cells were grown in bulk fastest growers were preferentially selected for. The degree of mutagenesis can be controlled by changing the parameters such as UV exposure times or using different lethal dosages (Nakanishi and Deuchi, 2013; Kamath *et al*., 2008; Tripathi *et al*., 2001). Thus, strain improvement could be achieved as a strategy for cost-effective production of astaxanthin.

5 – CONCLUSION & FUTURE PERSPECTIVES

With the fulfilment of this thesis work, useful information could be provided to the company A4F, which will be able to design new plans of study based on the information gathered in the present work.

The work performed allowed to select, among seven *H. pluvialis* strains, from the culture collection of A4F company, two strains with a superior performance (HP_02 and HP_03), that presented the characteristics more profitable to produce at a large scale. Depending on the cultivation conditions, those strains had the fastest growth rate of about 0.50 – 0.60 day^{-1}, were able to accumulate astaxanthin corresponding to 3.5 % - 4.5 % of their DW and also showed a global astaxanthin productivity (24 day in production), of about 1.60 – 1.90 $mg.g^{-1}$ $DW.day^{-1}$. These results are consistent with those of most of currently known strains. Regarding the saline stress assay, it only had significant results for HP_01 strain, which had an increase of 36 % in its astaxanthin content.

A gap remains between the FCM methods established for microalgae and their exploitation for the monitoring, development and optimization of biotechnological production processes. The multiparametric flow cytometric approach, was useful for the study of *H. pluvialis* cultures evolution, providing physiological information at an individual cell level. The specific advantage of using flow cytometry to analyze microalgae is the autofluorescence of naturally occurring intracellular pigments, which can be employed to distinguish between microalgae and other microorganisms. The chlorophyll autofluorescence was selected as the trigger for data collection, allowing to analyze only the *H. pluvialis* populations and reducing the bac*kg*round present in the samples such as debris and bacteria. Flow cytometry measurements revealed to be a methodology that can contribute efficiently to microalgae biotechnology development, representing a valuable survey analytical tool for a better exploitation of microalgae as feedstock for astaxanthin production. A strong correlation was observed between astaxanthin autofluorescence intensity measured by flow cytometry and astaxanthin content determined by pigment analysis in spectrophotometer.

Flow cytometry provides information on the intrinsic heterogeneity of a population. The distribution of different cell features in the population of a single species is influenced by culture conditions, the phase of cell cycle and mutations. The information gained on heterogeneity could therefore be exploited in combination with cell sorting to isolate cells overproducing a target compound. In the context of this thesis, seven strains were characterized throughout the growth vegetative stage and the induction stage at different physiological levels and the populations presented homogeneous, therefore it was not possible to make precise cell sorting, due to the inability to track and monitor the selected cells; consequently, it was a significant limitation.

In order to obtained heterogeneous strains, a preliminary assay using UV-C radiation exposure was performed to promote random mutagenesis. Results showed that biomass productivity at growth vegetative stage were similar to the values previous obtained and astaxanthin content increased at the end of the induction stage. In HP_03 strain, the only under this treatment, increased 32 % of its astaxanthin content, showing the importance that this previous treatment might have in the productivity of tested strains. Therefore, this technique could affect positively just a reduce number of cells in the population. Taking this into account, the screening of the mutants generated is crucial for the detection and selection of the cells that will accomplish astaxanthin overproduction.

Considering all the results obtained in this work, the production of astaxanthin is both important and challenging in *H. pluvialis* and so, it is essential that further studies continue to be developed in order to shed a new light into this matter. As future perspectives, in order to reduce the costs and maximize the high-value product production, strain improvement must be combined with the optimization of cultivation systems, making the production of *H. pluvialis* a process economically competitive with the synthetic production. Tests should be performed to elucidate if salinity stress can increase the astaxanthin productivity, such as the use of NaCl in the beginning of the induction phase. Also, UV mutagenesis presented itself to be an effective mutant agent to improve the strains of *H. pluvialis*, without the MGM legislation obstacle for human consumption. To sum up, new experimental designs may be defined to further explore this capacity and improve *H. pluvialis* strains, applying flow cytometry to detected cells of interest and using an advanced cell sorting function for improve astaxanthin productivity.

6 – REFERENCES

Aflalo C, Meshulam Y, Zarka A, Boussiba S. On the relative efficiency of two- vs. one-stage production of astaxanthin by the green alga *Haematococcus pluvialis. Biotechnol Bioeng* 2007;98:300–5.

Abdulqader G, Barsanti L, Tredici MR. Harvest of Arthrospira platensis from Lake Kossorom (Chad) and its household usage among the Kanembu. J Appl Phycol 2000;12:493-498.

Aberoumand A. A review article on edible pigments properties and sources as natural biocolorants in foodstuff and food industry. J of Dairy Food Sci 2011;6(1):71-78.

Aflalo C, Meshulam Y, Zarka A, Boussiba S. On the relative efficiency of two- vs. one-stage production of astaxanthin by the green alga *Haematococcus pluvialis. Biotechnol Bioeng* 2007;98:300–5.

Alvensleben N, Magnusson M, Heimann K. Salinity tolerant of four fresh microalgal species and the effects of salinity and nutrient limitation on biochemical profiles. J Appl Phycol 2016;28:861-887.

Ambati RR, Phang SM, Ravi S, Aswathanarayana RG. Astaxanthin: Sources, Extration, Stability, Biological activities and Its Commercial Applications – A Review. Mar Drugs 2014;12:128-152.

Basu S, Campbell HM, Dittel BN, Ray A. Purification of Specific Cell Population by Fluorescence Activated Cell Sorting (FACS). J Vis Exp 2010;41:e1546.

Bharathiraja B, Chakravarthy M, Praveen Kumar R, Yogendran D, Yavaraj D, Jayamuthunagai J, Praveen Kumar R, Palani S. Aquatic biomass (algae) as a future feed stock for bio-refineries: A review on cultivation, processing and products. Renewable and Sustainable Energy Rev 2015;47:634-653.

BCC Research http://www.bccresearch.com/pressroom/fod/global-carotenoids-market-reach-$1.4-billion-2018; Accessed: 18-Jul_2016.

Ben-Amotz A, Avron M. The potential use of *Dunaliella* for the production of glycerol, B-carotene and high-protein feed. In: San-Pietro A (ed.), Biosaline research: A look to the future. Plenum Pub Corp 1982;207–214.

Benavente-Valdés JR, Aguilar C, Contreras-Esquivel JC, Méndez-Zavala A, Montañez J. Strategies to enhance the production of photosynthetic pigments and lipids in chlorophycae species. Biotechnol Rep 2016;10:117-125.

Bhosale P. Environmental and cultural stimulants in the production of carotenoids from microorganisms. Appl Microbiol Biotechnol 2004;63:351-361.

Borowitzka MA. High-value products from microalgae—Their development and commercialization. J Appl Phycol 2013;25:743–756.

Borowitzka MA, Huisman JM, Osborn A. Culture of the astaxanthin-producing green alga *Haematococcus pluvialis*. J Appl Phycol 1991;3:295-304.

Boussiba S. Carotenogenesis in the green alga *Haematococcus pluvialis*: cellular physiology and stress response. Physiol. Plantarum 2000;108:111–117.

Boussiba S, Bing W, Yaun JP, Zarka A, Chen F. Changes in pigments profile in the green alga *Hameatococcus pluvialis* exposed to environmental stresses. Biotecchnol lett 1999;21:601-604.

Boussiba S, Vonshak A. Astaxanthin accumulation in the green alga *Haematococcus pluvialis*. Plant Cell Physiol 1991;32:1077-1082.

Cabanelas ITD, Zwart M, Kleinegris DMM, Barbosa MJ, Wijffels RH. Rapid method to screen and sort lipid accumulation microalgae. Bioresour Technol 2015;184:47-52.

Cellamare M, Rolland A, Jacquet S. Flow cytometry sorting of freshwater phytoplankton. J Appl Phycol 2010;22:87-100.

Chekanov K, Lobakova E, Selyakh I, Semenova L, Sidorov R, Solovchenko, A. Accumulation of astaxanthin by a new *Haematococcus pluvialis* strain BM1 from the White Sea coastal rocks (Russia). Mar Drugs 2014;12:4504–4520.

Chen Y, Li D, Lu W, Xing J, Hui B, Han Y. Screening and characterization of astaxanthin-hyperproducing mutants of *Haematococcus pluvialis. Biotechnol Lett* 2003;25:527–529.

Cheng J, Li K, Yang Z, Zhou J, Cen K. Enhancing the growth rate and astaxanthin yield of *Haematococcus pluvialis* by nuclear irradiation and high concentration of carbon dioxide stress. Bioresour Technol 2016;204:49-54.

Choi SL, Suh IS, Lee CG. Lumostatic operation of bubble column photobioreactors for *Haematococcus pluvialis* cultures using a specific light uptake rate as a control parameter. Enzyme Microbial Technol 2003;33:403-409.

Choi YE, Yun YS, Park JM, Yang JW. Determination of the time transferring cells for astaxanthin production considering two-stage process of *Haematococcus pluvialis* cultivation. Biosour Technol 2011;102:11249-11253.

Collins AM, Jones HDT, Han d, Hu Q, Beechem TE, Timlin JA. Carotenoid distribution in living cells of *Haematococcus pluvialis* (Chlorophyceae). PLoS ONE 2011;6(9).

Costa L, Brissos V, Lemos F, Ribeiro FR, Cabral JMS. Following Multi-Component Reactions in Liquid Medium Using Spectral Band-Fitting Techniques. Appl Spectroscopy 2008;62(8):1-7.

Crosbie ND, Pockl M, Weisse T. Rapid establishment of clonal isolated of freshwater autotrophic picoplankton by single-cell and single-colony sorting. J Microbiol Methods 2003;55:361-370.

Damiani Mc, Leonardi PL, Pieroni OI, Cáceres EJ. Ultrastructure of the cyst wall of *Haematococcus pluvialis* (Chlorophyceae): wall development and behaviour during cyst germination. Phycologia 2006;45(6):616-623.

Del Campo JA, Rodríguez H, Moreno J, Vargas MA, Rivas J, Guerrero MG. Accumulation of astaxanthin and lutein in *Chlorella zofingiensis* (Chlorophyta). Appl Microbiol Biotechnol 2004;64(6):848–54.

Del Rio E, Acien FG, Garcia-Malea MC, Rivas J, Del Rio E, Acien FG, *et al*., Efficient one-step production of astaxanthin by the microalga *Haematococcus pluvialis* in continuous culture. Biotechnol Bioeng 2005;91:808-815.

Del Rio E, Acien FG, Garcia-Malea MC, Rivas J, Molina-Grima E, Guerrero MG. Efficiency assessment of the one-step production of astaxanthin by the microalga *Haematococcus pluvialis*. Biotechnol Bioeng 2007;100:397–402.

Demirbas MF. Biofuels from algae for sustainable development. Appl Energy 2011;88:3473-3480.

Díaz M, Herrero M, García LA, and Quirós C. Application of flow cytometry to industrial microbial bioprocesses. Biochem Eng J 2010;48(3):385-407.

Doan TTY, Obbard JP. Enhanced intracellular lipid in *Nannochlotopsis* sp. Via random mutagenesis and flow cytometry cell sorting. Alga Res 2012;1:17-21.

Dominguez-Bocanegra AR, Legarreta IG, Jeronimo FM, Campocosio AT. Influence of environmental and nutritional factors in the production of astaxanthin from *Haematococcus pluvialis*. Bioresour Technol 2004;92: 209–214.

Elliot AM. Morphology and life history of *Haematococcus pluvialis*. Arch Protistenk 1934;82: 250–272.

Enzing C, Ploeg M, Barbosa M, Sijtsma L. Microalgae-based products for the food and feed sector: an outlook for Europe. JRC Scientific and Policy Reports 2014.

Fábregas J, Domínguez A, Álvarez DG, Lamela T, Otero A. Induction of astaxanthin accumulation by nitrogen and magnesium deficiencies in *Haematococcus pluvialis*. Biotechnol Lett 1998;20(6):623-626.

Fábregas J, Domínguez A, Regueiro M, Maseda A, Otero A. Optimization of culture medium for the continuous cultivation of the microalga *Haematococcus pluvialis*. Appl Microbiol Biotechnol 2000;53:530–535.

Fábregas J, Otero A, Maseda A, Domínguez A. Two-stage cultures for the production of astaxanthin from *Haematococcus pluvialis*. J Biotechnol 2001;89:65–71.

Forján E, Navarro F, Cuaresma M, Vaquero I, Ruíz-Domínguez MC, Gojkovic Z, *et al*. Microalgae: fast-growth sustainable green factories. Crit Rev Environ Sci Technol 2015;45:1705–1755.

Gacheva G, Dimitrova P, Pilarski P. New strain *Haematococcus* cf. *pluvialis* Rozhen-12 - growth, biochemical characteristics and future perspectives. Genetics and Plant Physiology 2015;5(1):29–38.

Gao Z, Meng C, Chen YC, Ahmed F, Mangott A, Schenk PM. Comparison of astaxanthin accumulation and biosynthesis gene expression of three *Haematococcus pluvialis* strains upon salinity stress. J Appl Phycol 2015;27:1853-1860.

García-Malea MC, Acién FG, Fernández JM, Cerón Mc, Molina E. Continuous production of green cells of *Haematococcus pluvialis*: Modeling of the irradiance effect. Enzyme and Microbial Technol 2006;38:981-989.

García-Malea MC, Brindley C, Del Río E, Acién FG, Fernández JM, Molina E. Modelling of growth accumulation of carotenoids in *Haematococcus pluvialis* as a function of irradiance and nutrientes supply. Biochem Eng J 2005;26:107-114.

González MA, Cifuentes AS, Gómez PI. Growth and totalcarotenoid content in four Chilean strains of *Haematococcus pluvialis* Flotow, under laboratory conditions. Gayana Bot 2009;66(1):58-70.

Goswami G, Chaudhuri S, Duttan D. The present perspective of astaxanthin with reference to biosynthesis and pharmacological importance. J Microbiol Biotechnol 2010;26:1925-1939.

Grewe C, Griehl C. Time- and media-dependent secondary carotenoid accumulation in *Haematococcus pluvialis*. Biotechnol J 2008;3:1232-1244.

Guedes AC, Amaro HM, Malcata FX. Microalgae as sources of carotenoids. Mar. Drugs. 2011;9:625–644.

Guerin M, Huntley ME, Olaizola M. *Haematococcus* astaxanthin: applications for human health and nutrition. Trends Biotechnol 2003;21:210–216.

Gwak Y, Hwang Y, Wang B, Kim M, Jeong J, Lee CG, Hu Q, Han D, Jin E. Comparative analyses of lipidomes and transcriptomes reveal a concerted action of multiple defensive systems against photooxidative stress in *Haematococcus pluvialis*. J Exp Botany 2014;65(15):4317-4334.

Habib MAB, Parvin M, Huntington TC, Hasan MR. A review of culture, production and use of *Spirulina* as food for humans and feeds for domestic animals and fish. FAO Fisheries and Aquaculture Circular 2008.

Hagen C, Siegmund S, Braune W. Ultrastructural and chemical changes in the cell wall of *Haematococcus pluvialis* (Volvocales, Chlorophyta) during aplanospore formation. Eur J Phycol 2002;37:217–226.

Han D, Li Y, Hu Q. Astaxanthin in microalgae: pathways, function and biotechnological implications. Algae 2013;28(2)131-147.

Hata N, Ogbonna JC, Hasegawa Y, Taroda H, Tanaka H. Production of astaxanthin by *Haematococcus pluvilis* ina sequential heterotrophic-photoautotrophic culture. J Appl Phycol 2001;13:395-402.

Higuera-Ciapara I, Felix-Valenzuela L, Goycoolea F. Astaxanthin: A Review of its Chemistry and Applications. Crit Rev Food Sci Nutr 2006;46:185–196.

Hyka P, Lickova S, Pribyl P, Melzoch K, Kovar K. Flow cytometry for the development of biotecnological processes with microalgae. Biotechnol Adv 2013;31:2-16.

Imamoglu E, Dalay MC, Sukan FV. Influences of different stress media and high light intensities on accumulation of astaxanthin in the green alga Haematococcus pluvialis. New Biotechnol 2009;26:199-204.

Kaewpintong K, Shotipruk A, Powtongsook, Pavasant P. Photoautotrophic high-density cultivation of vegetative cells of *Haematococcus pluvialis* in airlift bioreactor. Biosour Technol 2007;98:288-295.

Kamath BS, Vidhyavathi R, Sarada R, Ravishankar GA. Enhancement of carotenoids by mutation and stress induced carotenogenic genes in *Haematococcus pluvialis*. Biosour Technol 2008;99:8667-8673.

Kidd P. Astaxanthin, Cell Membrane Nutrient with Diverse Clinical Benefits and Anti-Aging Potential. Alternative Medicine Rev 2011;16:355-364.

Klochkova TA, Kwak MS, Han JW, Motomura T, Nagasato C, Kim GH. Cold-tolerant strain of *Haematococcus pluvialis* (Haematococcaceae, Chlorophyta) from Blomstrandhalvoya (Svalbard). Algae 2013;28:185-192.

Kobayashi M, Kakizono T, Yamaguchi K, Nishio N, Nagai S. Growth and astaxanthin formation of *Haematococcus pluvialis* in heterotrophic and mixotrophic conditions. J Ferment Bioeng 1992;74:61-63.

Kobayashi M, Kurimura Y, Tsuji Y. Morphological changes in the life cycle of green alga *Haematococcus pluvialis.* J Fermentation and Bioeng 1997a;84(1):94–97.

Kobayashi M, Kurimura Y, Tsuji Y. Light independent, astaxanthin production by the green microalga *Haematococcus pluvialis* under salt stress. Biotechnol 1997b;19:507–509.

Krujatz F, Lode A, Bruggemeier S, Schutz K, Framer J, Bley T, Gelinsky M, Weber J. Green bioprinting: Viability and growth analysis of microalgae immobilized in 3D-plotted hydrogels versus suspension cultures. Eng Life Sci 2015;00:1-11.

Lemoine Y, Schoefs B. Secondary ketocarotenoid astaxanthin biosynthesis in algae: a multifunctional response to stress. Photosynth Res 2010;106:155-177.

Li J, Zhu DL, Niu JF, Shen SD, Wang GC. An economic assessment of astaxanthin production by large scale cultivation of *Haematococcus pluvialis*. Biotechnol Adv 2011;29:568–574.

Li Y, Sommerfeld M, Chen F, Hu Q. Consumption of oxygen by astaxanthin biosynthesis: A protective mechanism against oxidative stress in *Haematococcus pluvialis* (Chlorophyceae). J Appl Phycol 2008;165:1783–1797.

López MCGM, Sánchez EDR, López JLC, Sevilla JMF, Rivas J, Guerrero MG, Grima EM. Comparative analysis of outdoor culture of *Haematococcus pluvialis* in tubular and bubble column photobioreactors. J of Biotechnol 2006; 123:329-342.

Lorenz RT. A Technical Review of *Haematococcus* Algae; NatuRose™ Technical Bulletin #060; Cyanotech Corporation 1999;1–12.

Lorenz RT, Cysewski, GR. Commercial potential for *Haematococcus* microalgae as a natural source of astaxanthin. Trends Biotechnol 2000;18:160–167.

Lu Y, Jiang P, Liu S, Gan Q, Cui H, Qin S. Methly jasmonate or gibberellins A_3-induced astaxanthin accumulation is associated with up-regulation of transcription of β-carotene ketolase genes (*bkts*) in microalga *Haematococcus pluvialis*. Bioresour Technol 2010;101:6468-6474.

Markou G, Nerantzis E. Microalgae for high-value compounds and biofuels production: A review with focus on cultivation under stress conditions. Biotechnol Advan 2013;31:1532-1542.

Mata TM, Martins AA, Caetano NS. Microalgae for biodiesel production and other applications: A review. Renewable and Sustainable Energy Rev 2010;14:217-232.

Milledge JJ. Commercial application of microalgae other than as biofuels: a brief review. Rev Environ Sci Biotechnol 2011;10:31-41.

Miki W. Biological functions and activities of animal carotenoids. Pure Appl Chem 1991;63:141–146.

Minhas AK, Hodgson P, Barrow CJ, Adholeya A. A review on the assessment of stress conditions for simultaneous production of microalgal lipids and carotenoids. Front Microbiol 2016;7:546

Nakanishi K, Deuchi K. Culture of a high-chlorophyll-producing and halotolerant Chlorella vulgaris. J Biosci Bioeng 2014;117(5):617-619.

Nigam PS, Luke JS. Food additives: Production of microbial pigments and their antioxidant properties. Current Opinion in Food Sci 2016;7:93-100.

Olaizola M. Commercial development of microalgal biotechnology: from the test tube to the marketplace. Biomol Eng 2003;20:459–466.

Orosa M, Valero J, Herrero C, Abalde J. Comparison of the accumulation of astaxanthin in *Haematococcus pluvialis* and other green microalgae under N-starvation and high light conditions. Biotechnol Let 2001;23: 1079-1085.

Pappas D, Wang K. Cellular separations: A review of new challenges in analytical chemistry. Analytica Chimica Acta 2007;601:26-35.

Park JC, Choi SP, Hong ME, Sim SJ. Enhanced astaxanthin production from microalga, *Haematococcus pluvialis* by two-stage perfusion culture with stepwise light irradiation. Bioprocess Biosyst Eng 2014;37:2039–2047.

Pashkow FJ, Watumull DG, Campbell CL. Astaxanthin: A Novel Potential Treatment for Oxidative Stress and Inflammation in Cardiovascular Disease. Am J Cardiol 2008;101:58D-68D.

Pereira H, Barreira L, Mozes A, Florindo C, Polo C, Duarte CV, Custódio L, Varela J. Microplate-based high throughput screening procedure forisolation of lipid-rich marina microalgae. Biotechnol Biofuels 2011;4:1-12.

Podola B, Li T, Melkonian M. Porous Substrate Biorectors: A Paradigm shift in Microalgal Biotechnology?. Trends Biotechnol 2016:in press.

Pringsheim EG. Nutritional requirements of *Haematococcus pluvialis* and related species. J Phycol 1966;2:1–7.

Proctor VW. Some controlling factors in the distribution of *Haematococcus pluvialis*. Ecology 1957;38:457–462.

Pulz O, Gross W. Valuable products from biotechnology of microalgae. Appl Microbiol Biotechnol 2004;65:635-648.

Raheem A, Azlina WA*KG*W, Yap YHT, Danquah MK. Thermochemical conversion of microalgal biomass for biofuel production. Renewable and Sustainable Energy Reviews 2015;49:990-999.

Recht L, Zarka A, Boussiba S. Patterns of carbohydrate and fatty acid changes under nitrogen starvation in the microalgae *Haematococcus pluvialis* and *Nannochloropsis* sp.. Appl Microbiol Biotechnol 2012;94:1495–1503.

Rioboo C, Barreiro ÓG, Abalde J, Cid Á. Flow cytometric analysis of the encystment process induced by paraquat exposure in *Haematococcus pluvialis* (Chlorophyceae). Eur J phycol 2011;46(2):89-97.

Safi C, Zebib B, Merah O, Pontalier PY, Garcia CV. Morphology, composition, production, processing and applications of *Chlorella vulgaris*: A review. Renewable and Sustainable Energy Reviews 2014;35:265-278.

Saha, SK, McHugh E, Hayes J, Moane S, Walsh D, Murray P. Effect of various stress regulatory factors on biomass and lipid production in microalga *Haematococcus pluvialis*. Bioresour Technol 2013;128:118–124.

Sarada R, Bhattacharya S, Ravishankar GA. Optimization of culture conditions for growth of the green alga

Haematococcus pluvialis. World J Microbiol Biotechnol 2002a;18:517–521.

Sarada R, Tripathi U, Ravishankar GA. Influence of stress on astaxanthin production in *Haematococcus pluvialis* grown under different culture conditions. Process Biochem 2002b;37:623– 627.

Sensen CW, Heimann K, Melkonian M. The production of clonal and axenic cultures of microalgae using fluorescence-activated cell sorting. Eur J Phycol 199;28:93-97.

Shah MMR, Liang Y, Cheng JJ, Daroch M. Astaxanthin-Producing green microalga *Haematococcus pluvialis*: from single cell to high value commercial products. Front Plant Sci 2016;7:531.

Sharon-Gojman R, Maimon E, Leu S, Zarka A, Boussiba S. Advanced methods for genetic engineering of *Haematococcus pluvialis* (Chlorophyceae, Volvocales). Algal Research 2015;10:8-15.

Singh J, Saxena RC. An Introduction to Microalgae: Diversity and Significance. Handbook of Marina Microalgae 2015;2:11-24.

Sinigalliano CD, Winshell J, Guerrero MA, Scorzetti G, Fell JW, Eaton RW, Brand L, Rein KS. Viable cell sorting of dinoflagellates by multiparametric flow cytometry. Phycologia 2009;48(4):249-257.

Sipaúba-Tavares LH, Millan RN, Berchielli-Morais FA. Effects of some parameters in upscale culture of Haematococcus pluvialis Flotow. Braz J Biol 2013;73(3):585-591.

Spolaore P, Joannis-Cassan C, Duran E, Isambert A. Commercial Applications of Microalgae. J Biocien and Bioeng 2006;101(2):87-96.

Steinbrenner J, Linden H. Regulation of Two Carotenoid Biosynthesis Genes Coding for Phytoene Synthase and Carotenoid Hydroxylase during Stress-Induced Astaxanthin Formation in the Green Alga *Haematococcus pluvialis*. Plant Physiol 2001;125:810-817.

Steinbrenner J, Linden H. Light induction of carotenoid biosynthesis genes in the green alga *Haematococcus pluvialis*: regulation by photosynthetic redox control. Plant Molecular Biology 2003;52:343-356.

Strittmatter M, Guerra T, Silva J, Gachon CMM. A new flagellated dispersion stage in *Paraphysoderma sedebokerense*, a pathogen of *Haematococcus pluvialis*. J Apply Phycol 2016;28:1553-1558.

Su Y, Wang J, Shi M, Niu X, Yu X, Gao L, Zhang X, Chen L, Zhang W. Metabolomic and network analysis of astaxanthin-producing *Haematococcus pluvialis* under various stress conditions. Bioresour Technol 2014;170:522–529.

Suyono EA, Aminin, Pradani L. Um'avatun U, Habiba RN, Ramdaniyah, Rohma EF. Combination of bue, red, white, and ultraviolet lights for increasing carotenoids and biomass of Microalga Haematococcus pluvialis. Procedia Environ Sci 2015;28:399-405.

Tam LT, Hoang DD, Ngoc Mai DT, Hoai Thu NT, Lan Anh HT, Hong DD. Study on the effect of salt concentration on growth and astaxanthin accumulation of microalgae *Haematococcus pluvialis* as the initial basis for two phase culture of astaxanthin production. Tap Chi Sinh Hoc 2012;34:213–223.

Terashima M, Freeman ES, Jinkerson RE, Jonikas MC. A fluorescence-activated cell sorting-based strategy for rapid isolation of high-lipid Chlamydomonas mutants. Plant J 2015;81:147-159.

Tjahjono AE, Hayama Y, Kakizono T, Terada Y, Nishio N, Nagai S. Hyper-accumulation of astaxanthin in a green alga *Haematococcus pluvialis* at elevated temperatures. Biotechnol Lett 1994;16(2):133-138.

Tocquim P, Fratamico A, Franck F. Screening for a low-cost *Haematococcus pluvialis* medium reveals an unexpected impact of a low N/P ratio on vegetative growth. J Appl Phycol 2012;24:365-373.

Tran HL, Lee KH, Hong CH. Effects of LED irradiation on the growth and Astaxanthin Production of *Haematococcus pluvialis*. Biocienc Biotec R Asia 2015;12(2):1167-1173.

Triki A, Maillard P, Gudin C. Gametogenesis in *Haematococcus pluvialis* Flotow (Volvocales, Chlorophyta). Phycologia 1997;36:190–194.

Tripathi U, Venkateshwaran G, Sarada R, Ravishankar GA. Studies on *Haematococcus pluvialis* for improved production of astaxanthin by mutagenesis. World J Microbiol Biotechnol 2001;17:143–148.

Tuli HS, Chaudhary P, Beniwal V, Sharma AK. Microbial pigments as natural color sources: current trends and future perspectives. J Food Sci Technol 2014.

Vassilev SV, Vassileva CG. Composition, properties and challenges of algae biomass for biofuel application: An overview. Fuel 2016;181:1-33.

Vidhyavathi R, Venkatachalam L, Sarada R, Ravishankar GA. Regulation of carotenoid biosynthetic genes expression and carotenoid accumulation in the green alga *Haematococcus pluvialis* under nutrient stress conditions. J Exp Bot 2008;59(6):1409–1418.

Vigani M, Parisi C, Rodríguez-Cerezo E, Barbosa MJ, Sijtsma L, Ploeg M, Enzing C. Food and feed products from microalgar: Market opportunities and challenges for EU. Food Science and Techno 2015;42:81-92.

Vigeolas H, Duby F, Kaymak E, Niessen G, Motte P, Franck F, Remacle C. Isolation and partial characterization of mutants with elevated lipid content in *Chlorella sorokiniana* and *Scenedesmus obliquus*. J Biotechnol 2012;162:3-12.

Wahby I, Bennis I, Tilsaghani C, Lubián LM. Potential use of flow cytometry in microalgae-based biodiesel project development. J Innova Apply Studies 2014;5(4):333-343.

Wan M, Zhang J, Hou D, Fan J, Li Y, Huang J, Wang J. The effect of temperature on cell growth and astaxanthin accumulation of *Haematococcus pluvialis* during a light–dark cyclic cultivation. Bioresour Technol 2014;167:276-283.

Wayama M, Ota S, Matsuura H, Nango N, Hirata A., Kawano S. Three-dimensional ultrastructural study of oil and astaxanthin accumulation during encystment in the green alga *Haematococcus pluvialis*. PLoS ONE 2013;8.

Wen Z, Liu Z, Hou Y, Liu C, Gao F, Zheng Y, Chen F. Ethanol induced astaxanthin accumulation and transcriptional expression of carotenogenic genes in *Haematococcus pluvialis*. Enzyme and Microbial Technol 2015;78:10-17.

Yamashita E. Astaxanthin as a Medical Food. Functional Foods in Health and Disease 2013;3(7):254-258.

Yuan JP, Peng J, Yin K, Wang JH. Potential health promoting effects of astaxanthin: A high-value carotenoid mostly from microalgae. Mol Nutr Food Res 2011;55:150–165.

Xie B, Stessman D, Hart JH, Dong H, Wang Y, Wright DA, Nikolau BJ, Spalding MH, Halverson LJ. High-throughput fluorescence-activated cell sorting for lipid hyperaccumulating *Chlamydomonas reinhardtii* mutants. Plant Biotechnol J 2014;12:872-882.

Zhang W, Wang J, Wang J, Liu T. Attached cultivation of *Haematococcus pluvialis* for astaxanthin production. Bioresour Technol 2014;158:329–335.

Zhang Z, Wang B, Hu Q, Sommerfeld M, Li Y. A new paradigm for producing astaxanthin from unicellular green alga *Haematococcus pluvialis*. Biotechnol Bioeng 2016;9999:1-12.

Zhao Y, Shang M, Xu JW, Zhao P, Li T, Yu X. Enhanced astaxanthin production from a novel strain of *Haematococcus pluvialis* using fulvic acid. Process Biochem 2015;50:2072-2077.

Zhekisheva M, Boussiba S, Khozin-Goldberg I, Zarka A, Cohen Z. Accumulation of oleic acid in *Haematococcus pluvialis* (Chlorophyceae) under nitrogen starvation or high light is correlated with that of astaxanthin esters. J Phycol 2002;38:325– 331.